CHAPTER THIRTEEN

Compressible Flows via Finite Element Methods

In this chapter, finite element analyses of both inviscid and viscous compressible flows are examined. Traditionally, computational schemes for compressible inviscid flow are developed separately from compressible viscous flows, governed by Euler equations and Navier-Stokes system of equations, respectively. However, it is our desire in this chapter to study numerical schemes capable of treating a compressible flow with or without the effect of viscosity or diffusion. Furthermore, it would be desirable to develop a scheme that can handle all speed regimes – not only the compressible flow, but the incompressible flow as well. To accomplish this goal, the most suitable governing equations to use are the Navier-Stokes system of equations written in conservation form in terms of conservation variables. Advantages of transforming the conservation variables into entropy variables and primitive variables will be explored. One of the most prominent features in compressible flow calculations is the ability of numerical schemes to resolve shock waves or discontinuities in high-speed flows. Furthermore, compressible viscous flows at high Mach numbers and high Reynolds numbers lead to significant numerical difficulties. We shall address these and other issues in this chapter.

To this end, we begin with the general description of the governing equations in Section 13.1, followed by the Taylor-Galerkin methods (TGM), generalized Galerkin methods (GGM), generalized Petrov-Galerkin (GPG) methods, characteristic Galerkin methods (CGM), and discontinuous Galerkin methods (DGM) in Sections 13.2 through 13.4. Finally, the flowfield-dependent variation (FDV) methods introduced in FDM and discussed earlier in Section 6.5 will be presented for FEM applications (Section 13.6). This subject will be treated again in Chapter 16, where many of the methods in both FDM and FEM can be shown to be the special cases of FDV methods.

13.1 GOVERNING EQUATIONS

So far in the previous chapters, we have dealt with Stokes flows (no convection terms, Section 10.1.4), Burgers' equations (with convective terms but without pressure gradients, Chapter 11), and incompressible flows (with continuity and momentum equations, Chapter 12). More general types of flows include compressibility or density variations as a function of space and time and in nonisothermal environments, which are characterized by the Navier-Stokes system of equations for conservation of mass, momentum,

and energy. Although we discussed these equations in Chapters 2 and 6, we shall repeat them here for convenience.

Continuity Equation

$$\frac{\partial \rho}{\partial t} + (\rho \mathbf{v}_i)_{,i} = 0 \tag{13.1.1a}$$

Momentum Equation

$$\rho \frac{\partial \mathbf{v}_j}{\partial t} + \rho \mathrm{v}_{j,i} \mathrm{v}_i + p_{,j} - \tau_{ij,i} - \rho F_j = 0 \tag{13.1.1b}$$

Energy Equation

$$\rho \frac{\partial \varepsilon}{\partial t} + \rho \varepsilon_{,i} \mathbf{v}_i + p \mathbf{v}_{i,i} - \tau_{ij} \mathbf{v}_{j,i} + q_{i,i} = 0 \tag{13.1.1c}$$

where τ_{ij}, ε, and q_i denote viscous stress tensor, internal energy, and heat flux, respectively.

Stress Tensor

$$\tau_{ij} = \mu \left(\mathrm{v}_{i,j} + \mathrm{v}_{j,i} - \frac{2}{3} \mathrm{v}_{k,k} \delta_{ij} \right)$$

Internal Energy

$$\varepsilon = c_p T - \frac{p}{\rho} = c_v T$$

Heat Flux

$$q_i = -kT_{,i}$$

where the dynamic viscosity μ and thermal conductivity k are given by Sutherland's law [(2.2.7) and (2.2.8)], respectively; and c_p and c_v represent specific heats at constant pressure and volume, respectively.

These equations may be combined into a conservation form

$$\frac{\partial \mathbf{U}}{\partial t} + \frac{\partial \mathbf{F}_i}{\partial x_i} + \frac{\partial \mathbf{G}_i}{\partial x_i} = \mathbf{B} \tag{13.1.2}$$

where $\mathbf{U}, \mathbf{F}_i, \mathbf{G}_i$, and $\mathbf{B}$ are the conservation variables, convection flux, diffusion flux, and body force vector, respectively.

$$\mathbf{U} = \begin{bmatrix} \rho \\ \rho \mathrm{v}_j \\ \rho E \end{bmatrix}, \quad \mathbf{F}_i = \begin{bmatrix} \rho \mathrm{v}_i \\ \rho \mathrm{v}_i \mathrm{v}_j + p \delta_{ij} \\ \rho E \mathrm{v}_i + p \mathrm{v}_i \end{bmatrix}, \quad \mathbf{G}_i = \begin{bmatrix} 0 \\ -\tau_{ij} \\ -\tau_{ij} \mathrm{v}_j + q_i \end{bmatrix}, \quad \mathbf{B} = \begin{bmatrix} 0 \\ \rho F_j \\ \rho F_j \mathrm{v}_j \end{bmatrix}$$

with E being the total energy,

$$E = \varepsilon + \frac{1}{2} \mathrm{v}_j \mathrm{v}_j \tag{13.1.3}$$

and the pressure p given by the equation of state,

$$p = \rho RT \tag{13.1.4a}$$

$$p = (\gamma - 1)\,\rho\left(E - \frac{1}{2}v_i v_i\right) \tag{13.1.4b}$$

$$T = \frac{1}{c_v}\left(E - \frac{1}{2}v_i v_i\right) \tag{13.1.4c}$$

where R is the specific gas constant which may be related to the specific heats as follows:

$$R = \frac{c_p(\gamma - 1)}{\gamma}, \qquad \gamma = \frac{c_p}{c_v}$$

The equation of state plays the role of a constraint for the Navier-Stokes system of equations.

For the purpose of generality, we shall keep the source terms **B** so that numerical formulations can be accommodated for the reacting flows as discussed in Chapter 22.

Nondimensional Form of Navier-Stokes System of Equations

The numerical solution of the Navier-Stokes system of equations in dimensional form typically involves operations between terms that vary by several orders of magnitude. This leads to a situation in which the numerical solution fails or becomes unstable as the computer floating point limits are exceeded. For this reason, the governing equations are often put into nondimensional form. Placing the flow variables in dimensionless form insures that variations are maintained within certain prescribed limits between 0 and l. Additionally, writing the Navier-Stokes system of equations in dimensionless form facilitates generalization to embody a large range of problems. Also, the dimensionless form has the advantage that characteristic parameters such as Mach number, Reynolds number. Prandtl number, etc., can be regulated independently. Toward this end, we introduce the nondimensional variables

$$\begin{aligned} x_i^* &= \frac{x_i}{L}, \qquad t^* = \frac{t}{L/v_\infty}, \qquad \rho^* = \frac{\rho}{\rho_\infty}, \qquad v_i^* = \frac{v_i}{v_\infty}, \qquad E^* = \frac{E}{v_\infty^2} \\ p^* &= \frac{p}{\rho_\infty v_\infty^2}, \qquad T^* = \frac{T}{T_\infty}, \qquad \mu^* = \frac{\mu}{\mu_\infty}, \qquad F_i^* = \frac{F_i}{v_\infty^2/L} \end{aligned} \tag{13.1.5}$$

where an asterisk denotes nondimensional variables, infinity represents freestream conditions, and L is the reference length used in the Reynolds number

$$\mathrm{Re} = \frac{\rho_\infty v_\infty L}{\mu_\infty} \tag{13.1.6}$$

With the nondimensional variables above, the dimensionless form of Navier-Stokes system of equations in conservation form (13.1.2) becomes

$$\frac{\partial \mathbf{U}^*}{\partial t^*} + \frac{\partial \mathbf{F}_i^*}{\partial x_i^*} + \frac{\partial \mathbf{G}_i^*}{\partial x_i^*} = \mathbf{B}^* \tag{13.1.7}$$

where the conservation flow variable vector, the convection flux vector, the diffusion

flux vector, and the source vector in nondimensional form are defined by

$$\mathbf{U}^* = \begin{bmatrix} \rho^* \\ \rho^* \mathrm{v}_j^* \\ \rho^* E^* \end{bmatrix}, \qquad \mathbf{F}_i^* = \begin{bmatrix} \rho^* \mathrm{v}_i^* \\ \rho^* \mathrm{v}_i^* \mathrm{v}_j^* + p^* \delta_{ij} \\ \rho^* E^* \mathrm{v}_i^* + p^* \mathrm{v}_i^* \end{bmatrix}, \qquad \mathbf{G}_i^* = \frac{1}{\mathrm{Re}} \begin{bmatrix} 0 \\ -\tau_{ij}^* \\ -\tau_{ij}^* \mathrm{v}_j^* + q_i^* \end{bmatrix},$$

$$\mathbf{B}^* = \begin{bmatrix} 0 \\ \rho^* F_j^* \\ \rho^* F_j^* \mathrm{v}_j^* \end{bmatrix}, \qquad \mathbf{b}_i = \frac{1}{\mathrm{Re}} \frac{\partial \mathbf{G}_i}{\partial \mathbf{U}}, \qquad \mathbf{c}_{ij} = \frac{1}{\mathrm{Re}} \frac{\partial \mathbf{G}_i}{\partial \mathbf{U}_j}$$

Here the nondimensional stagnation energy, the viscous stress tensor, and the thermal conductivity are

$$E^* = \frac{p^*}{(\gamma - 1)\rho^*} + \frac{1}{2} \mathrm{v}_j^* \mathrm{v}_j^* \tag{13.1.8}$$

$$\tau_{ij}^* = \mu^* \left(\mathrm{v}_{i,j}^* + \mathrm{v}_{j,i}^* - \frac{2}{3} \mathrm{v}_{k,k}^* \delta_{ij} \right) \tag{13.1.9}$$

$$k^* = \frac{\mu^*}{(\gamma - 1) M_\infty^2 \, \mathrm{Pr}} = \frac{k}{\mu_\infty V_\infty^2 / T} \tag{13.1.10}$$

with Sutherland's law in the nondimensional form,

$$\mu^* = \frac{1 + S_o / T_\infty}{T^* + S_o / T_\infty} (T^*)^{\frac{3}{2}} \tag{13.1.11}$$

and the freestream Mach number,

$$M_\infty = \frac{V_\infty}{\sqrt{\gamma(\gamma - 1) c_v T_\infty}} \tag{13.1.12}$$

The nondimensional equations of state (13.1.4b,c) become

$$p^* = (\gamma - 1)\rho^* \left(E^* - \frac{1}{2} \mathrm{v}_j^* \mathrm{v}_j^* \right), \quad E^* = c_v^* T^* = \frac{T^*}{\gamma(\gamma - 1) M_\infty^2} \tag{13.1.13}$$

or

$$T^* = \frac{1}{c_v^*} \left(E^* - \frac{1}{2} \mathrm{v}_j^* \mathrm{v}_j^* \right) \tag{13.1.14}$$

where the nondimensional specific heat at constant volume,

$$c_v^* = \frac{1}{\gamma(\gamma - 1) M_\infty^2}, \quad c_p^* = \frac{c_p}{\mathrm{v}_\infty^2 / T_\infty} = \frac{1}{(\gamma - 1) M_\infty^2} \tag{13.1.15}$$

An alternative form of the nondimensional state equations is expressed by

$$p^* = \rho^* R^* T^* \tag{13.1.16}$$

with

$$R^* = \frac{1}{\gamma M_\infty^2} \tag{13.1.17}$$

For convenience, the asterisks will now be omitted, but we continue to work with the dimensionless form of the governing equations in all or the following discussions.

13.2 TAYLOR-GALERKIN METHODS AND GENERALIZED GALERKIN METHODS

In Chapter 11, the Taylor Galerkin methods (TGM) were formulated by expanding the variables into Taylor series. It was also shown that similar results can be obtained from the generalized Galerkin methods (GGM) using the double projections of the residual onto the spatial and temporal test functions for the linearized Burgers' equations in which the numerical diffusion is absent. For the nonlinear Burgers' equations (Section 11.2.5), however, it was shown that TGM was capable of explicitly providing the numerical diffusion. In this section, we examine TGM as applied to the Navier-Stokes system of equations with the convection and diffusion fluxes transformed to the conservation variables through Jacobians. It will be shown that the numerical diffusion arises in much more complicated form than it does for the nonlinear Burgers' equations. We then discuss GGM, which is simpler but not as effective as TGM associated with convection-dominated flows or discontinuities. In Chapter 11 dealing with the Burgers equations, TGM was identified as a special case of GGM. This is no longer the case in this chapter working with the Navier-Stokes system of equations. This is because many different forms of TGM result from various approximations in Taylor series expansion of the conservation variables. We elaborate these and other topics below.

13.2.1 TAYLOR-GALERKIN METHODS

One of the well-known schemes in FEM as introduced in Chapter 11 is the Taylor-Galerkin methods (TGM) as applied to the Navier-Stokes system of equations. In dealing with the Navier-Stokes system of equations, unlike the Burgers' equations discussed in Chapter 11, it is convenient to work with conservation variables transformed from the convection and diffusion fluxes as follows [Hassan, Morgan, and Peraire, 1991]:

$$\frac{\partial \mathbf{F}_i}{\partial t} = \mathbf{a}_i \frac{\partial \mathbf{U}}{\partial t} \tag{13.2.1}$$

$$\frac{\partial \mathbf{G}_i}{\partial t} = \mathbf{b}_i \frac{\partial \mathbf{U}}{\partial t} + \mathbf{c}_{ij} \frac{\partial \mathbf{U}_{,j}}{\partial t} \tag{13.2.2}$$

with the convection Jacobian $\mathbf{a}_i$, diffusion Jacobian $\mathbf{b}_i$, and diffusion gradient Jacobian $\mathbf{c}_{ij}$ being defined as in (6.3.8).

Let us consider the Taylor series expansion of $\mathbf{U}^{n+1}$ in the form,

$$\mathbf{U}^{n+1} = \mathbf{U}^n + \Delta t \frac{\partial \mathbf{U}^n}{\partial t} + \frac{\Delta t^2}{2} \frac{\partial^2 \mathbf{U}^{n+1}}{\partial t^2} + \mathrm{O}(\Delta t^3) \tag{13.2.3}$$

in which the second derivative is set at the implicit form $(n+1)$. Substituting (13.1.2) into (13.2.3) gives

$$\Delta \mathbf{U}^{n+1} = \Delta t \left(-\frac{\partial \mathbf{F}_i}{\partial x_i} - \frac{\partial \mathbf{G}_i}{\partial x_i} + \mathbf{B} \right)^n + \frac{\Delta t^2}{2} \frac{\partial}{\partial t} \left(-\frac{\partial \mathbf{F}_i}{\partial x_i} - \frac{\partial \mathbf{G}_i}{\partial x_i} + \mathbf{B} \right)^{n+1} + \mathrm{O}(\Delta t^3) \tag{13.2.4}$$

Using the definitions of convection, diffusion, and diffusion gradient Jacobians, the temporal rates of change of convection and diffusion variables may be written as follows:

$$\begin{aligned}
\frac{\partial \mathbf{F}_i^n}{\partial t} &= \left(\mathbf{a}_i \frac{\partial \mathbf{U}}{\partial t}\right)^n = \left[\mathbf{a}_i\left(-\frac{\partial \mathbf{F}_j}{\partial x_j} - \frac{\partial \mathbf{G}_j}{\partial x_j} + \mathbf{B}\right)\right]^n \\
\frac{\partial \mathbf{F}_i^{n+1}}{\partial t} &= \mathbf{a}_i\left(-\frac{\partial \mathbf{F}_j^{n+1}}{\partial x_j} - \frac{\partial \mathbf{G}_j^{n+1}}{\partial x_j} + \mathbf{B}^{n+1}\right) \\
&= \mathbf{a}_i\left[\left(-\mathbf{a}_j \frac{\partial}{\partial x_j}(\mathbf{U}^{n+1} - \mathbf{U}^n) - \frac{\partial \mathbf{F}_j^n}{\partial x_j} - \frac{\partial \mathbf{G}_j^{n+1}}{\partial x_j} + \mathbf{B}^{n+1}\right)\right] \qquad (13.2.5) \\
\frac{\partial \mathbf{G}_i^{n+1}}{\partial t} &= \left(\mathbf{b}_i \frac{\partial \mathbf{U}}{\partial t}\right)^{n+1} + \left[\mathbf{c}_{ij} \frac{\partial}{\partial t}\left(\frac{\partial \mathbf{U}}{\partial x_j}\right)\right]^{n+1}
\end{aligned}$$

or

$$\frac{\partial \mathbf{G}_i^{n+1}}{\partial t} = \left(\mathbf{b}_i - \frac{\partial \mathbf{c}_{ij}}{\partial x_j}\right)\frac{\Delta \mathbf{U}}{\Delta t}^{n+1} + \frac{\partial}{\partial x_j}\left(\mathbf{c}_{ij}\frac{\Delta \mathbf{U}}{\Delta t}\right)^{n+1} \qquad (13.2.6)$$

Substituting (13.2.5) and (13.2.6) into (13.2.4) yields

$$\begin{aligned}
\Delta \mathbf{U}^{n+1} &= \Delta t\left(-\frac{\partial \mathbf{F}_i}{\partial x_i} - \frac{\partial \mathbf{G}_i}{\partial x_i} + \mathbf{B}\right)^n \\
&\quad + \frac{\Delta t^2}{2}\left\{\frac{\partial}{\partial x_i}\left[-\mathbf{a}_i\left(-\mathbf{a}_j \frac{\partial \Delta \mathbf{U}^{n+1}}{\partial x_j} - \frac{\partial \mathbf{F}_j^n}{\partial x_j} - \frac{\partial \mathbf{G}_j^{n+1}}{\partial x_j} + \mathbf{B}^{n+1}\right)\right.\right. \\
&\quad \left.\left. - \left(\mathbf{e}_i + \frac{\partial \mathbf{c}_{ij}}{\partial x_j}\right)\frac{\Delta \mathbf{U}^{n+1}}{\Delta t}\right] + \frac{\partial \mathbf{B}^{n+1}}{\partial t}\right\} \qquad (13.2.7)
\end{aligned}$$

with

$$\mathbf{e}_i = \mathbf{b}_i - \frac{\partial \mathbf{c}_{ij}}{\partial x_j}$$

Neglecting the spatial and temporal derivatives of $\mathbf{B}$, we rewrite (13.2.7) in the form

$$\begin{aligned}
&\left\{1 + \frac{\Delta t}{2}\frac{\partial \mathbf{e}_i}{\partial x_i} - \frac{\Delta t^2}{2}\frac{\partial}{\partial x_i}\left(\mathbf{a}_i \mathbf{a}_j - \frac{\mathbf{c}_{ij}}{\Delta t}\right)\frac{\partial}{\partial x_j}\right\}\Delta \mathbf{U}^{n+1} \\
&\quad = \Delta t\left(-\frac{\partial \mathbf{F}_i}{\partial x_i} - \frac{\partial \mathbf{G}_i}{\partial x_i} + \mathbf{B}\right)^n + \frac{\Delta t^2}{2}\frac{\partial}{\partial x_i}\left(\mathbf{a}_i \frac{\partial \mathbf{F}_j}{\partial x_j}\right)^n
\end{aligned}$$

Here the second derivatives of $\mathbf{G}_i$ are neglected and all Jacobians are assumed to remain constant within an incremental time step, but updated at subsequent time steps.

We now introduce the trial functions for the various variables in the form,

$$\mathbf{U} = \Phi_\alpha \mathbf{U}_\alpha, \qquad \mathbf{F}_i = \Phi_\alpha \mathbf{F}_{\alpha i}, \qquad \mathbf{G}_i = \Phi_\alpha \mathbf{G}_{\alpha i}, \qquad \mathbf{B} = \Phi_\alpha \mathbf{B}_\alpha$$

Substituting the above into (13.2.8) leads to an implicit scheme,

$$(A_{\alpha\beta}\delta_{rs} + B_{\alpha\beta rs})\Delta U_{\beta s}^{n+1} = H_{\alpha r}^n + N_{\alpha r}^{n+1} + \overline{N}_{\alpha r}^n \qquad (13.2.8)$$

where

$$A_{\alpha\beta} = \int_\Omega \Phi_\alpha \Phi_\beta d\Omega$$

$$B_{\alpha\beta rs} = \frac{\Delta t}{2}\int_\Omega e_{irs}\Phi_\alpha\Phi_{\beta,i}d\Omega + \frac{\Delta t^2}{2}\int_\Omega\left[\left(a_{irq}a_{jqs} - \frac{c_{ijrs}}{\Delta t}\right)\Phi_{\alpha,i}\Phi_{\beta,j}\right]d\Omega$$

$$H^n_{\alpha r} = \Delta t\int_\Omega\left[\Phi_{\alpha,i}\Phi_\beta\left(F^n_{\beta ir} + G^n_{\beta ir}\right) + \Phi_\alpha\Phi_\beta B^n_{\beta r} - \frac{\Delta t}{2}a_{irs}\Phi_{\alpha,i}\Phi_{\beta,j}F^n_{\beta js}\right]d\Omega$$

$$N^{n+1}_{\alpha r} = \frac{\Delta t^2}{2}\int_\Gamma\left(a_{irq}a_{jqs} - \frac{c_{ijrs}}{\Delta t}\right)\overset{*}{\Phi}_\alpha\Delta U^{n+1}_{s,j}n_i d\Gamma$$

$$\overline{N}^n_{\alpha r} = -\int_\Gamma\left[\Delta t\overset{*}{\Phi}_\alpha\left(F^n_{ir} + G^n_{ir}\right) - \frac{\Delta t^2}{2}a_{irs}\overset{*}{\Phi}_\alpha F^n_{js,j}\right]n_i d\Gamma$$

where the indices α, β denote the global node, r, s represent the equation number listed in (13.1.2), and i, j indicate spatial coordinates. Note also that all quantities with r, s are lightfaced, indicating that they are no longer vector quantities.

It should be recognized that the integral

$$\frac{\Delta t^2}{2}\int_\Omega \mathbf{a}_{irq}\mathbf{a}_{jsq}\Phi_{\alpha,i}\Phi_{\beta,j}d\Omega = \int_\Omega \nu_{ijrs}\Phi_{\alpha,i}\Phi_{\beta,j}d\Omega \tag{13.2.9}$$

contained in $B_{\alpha\beta rs}$ represents the numerical diffusion, corresponding to that given in (11.2.76) for the Burgers' equations. We note that the velocity components for the Burgers' equations are simply replaced by the convection Jacobian components for the Navier-Stokes system of equations.

Instead of simulating the second order time derivatives implicitly, we may leave them in an explicit form so that the standard Taylor series can be used.

$$\mathbf{U}^{n+1} = \mathbf{U}^n + \Delta t\frac{\partial\mathbf{U}^n}{\partial t} + \frac{\Delta t^2}{2}\frac{\partial^2\mathbf{U}^n}{\partial t^2} + \mathrm{O}(\Delta t^3) \tag{13.2.10}$$

where

$$\frac{\partial\mathbf{U}}{\partial t} = -\frac{\partial\mathbf{F}_i}{\partial x_i} - \frac{\partial\mathbf{G}_i}{\partial x_i} + \mathbf{B} = -\mathbf{a}_i\frac{\partial\mathbf{U}}{\partial x_i} - \frac{\partial\mathbf{G}_i}{\partial x_i} + \mathbf{B} \tag{13.2.11}$$

$$\frac{\partial^2\mathbf{U}}{\partial t^2} = -\frac{\partial}{\partial t}\left(\mathbf{a}_i\frac{\partial\mathbf{U}}{\partial x_i} + \frac{\partial\mathbf{G}_i}{\partial x_i} - \mathbf{B}\right)$$

or

$$\frac{\partial^2\mathbf{U}}{\partial t^2} = \frac{\partial}{\partial x_j}\left(\mathbf{a}_i\mathbf{a}_j\frac{\partial\mathbf{U}}{\partial x_i}\right) + \frac{\partial}{\partial x_i}\left(\mathbf{a}_i\frac{\partial\mathbf{G}_j}{\partial x_j}\right) - \frac{\partial}{\partial x_i}(\mathbf{a}_i\mathbf{B}) + \frac{\partial\mathbf{B}}{\partial t} \tag{13.2.12}$$

Substituting (13.2.11) and (13.2.12) into (13.2.10), we obtain

$$\Delta\mathbf{U}^{n+1} = \Delta t\left\{-\frac{\partial\mathbf{F}_i}{\partial x_i} - \frac{\partial\mathbf{G}_i}{\partial x_i} + \mathbf{B} + \frac{\Delta t}{2}\left[\frac{\partial}{\partial x_j}\left(\mathbf{a}_i\mathbf{a}_j\frac{\partial\mathbf{U}}{\partial x_i}\right) + \frac{\partial^2(\mathbf{a}_i\mathbf{G}_j)}{\partial x_i\partial x_j} - \frac{\partial}{\partial x_i}(\mathbf{a}_i\mathbf{B}) + \frac{\partial\mathbf{B}}{\partial t}\right]\right\}^n \tag{13.2.13}$$

or

$$\Delta\mathbf{U}^{n+1} = \Delta t\left(-\frac{\partial\mathbf{F}_i}{\partial x_i} - \frac{\partial\mathbf{G}_i}{\partial x_i} + \mathbf{B}\right)^n + \frac{\Delta t^2}{2}\left\{\frac{\partial}{\partial x_i}\left(\mathbf{a}_i\mathbf{a}_j\frac{\partial\Delta\mathbf{U}^{n+1}}{\partial x_j} + \mathbf{a}_i\frac{\partial\mathbf{F}^n_j}{\partial x_j}\right) + \frac{\partial^2(\mathbf{a}_i\mathbf{G}_j)^{n+1}}{\partial x_i\partial x_j} + \frac{\partial}{\partial x_i}(\mathbf{a}_i\mathbf{B})^{n+1} + \frac{\partial\mathbf{B}^{n+1}}{\partial t}\right\} \tag{13.2.14}$$

Rearranging (13.2.14) gives

$$\left[1-\frac{\Delta t^2}{2}\frac{\partial}{\partial x_i}\left(\mathbf{a}_i\mathbf{a}_j-\frac{\mathbf{c}_{ij}}{\Delta t}\right)\frac{\partial}{\partial x_j}\right]\Delta\mathbf{U}^{n+1}$$
$$=\Delta t\left(-\frac{\partial\mathbf{F}_i}{\partial x_i}-\frac{\partial\mathbf{G}_i}{\partial x_i}+\mathbf{B}\right)^n+\frac{\Delta t^2}{2}\frac{\partial}{\partial x_i}\left(\mathbf{a}_i\frac{\partial\mathbf{F}_j}{\partial x_j}\right)^n \tag{13.2.15}$$

where the second derivatives of $\mathbf{G}_i$ are assumed to be negligible and $\mathbf{B}$ is constant in space and time. We then arrive at an implicit finite element scheme,

$$(A_{\alpha\beta}\delta_{rs}+B_{\alpha\beta rs})\,\Delta U_{\beta s}^{n+1}=H_{\alpha r}^n+N_{\alpha r}^{n+1}+\overline{N}_{\alpha r}^n \tag{13.2.16}$$

where

$$A_{\alpha\beta}=\int_\Omega\Phi_\alpha\Phi_\beta\,d\Omega$$
$$B_{\alpha\beta rs}=\frac{\Delta t^2}{2}\int_\Omega\left[\left(a_{irq}a_{jqs}-\frac{c_{ijrs}}{\Delta t}\right)\Phi_{\alpha,i}\Phi_{\beta,j}\right]d\Omega$$
$$H_{\alpha r}^n=\Delta t\int_\Omega\left[\Phi_{\alpha,i}\Phi_\beta\left(F_{\beta ir}^n+G_{\beta ir}^n\right)+\Phi_\alpha\Phi_\beta B_{\beta r}^n-\frac{\Delta t}{2}a_{irs}\Phi_{\alpha,i}\Phi_{\beta,j}F_{\beta js}^n\right]d\Omega$$
$$N_{\alpha r}^{n+1}=\frac{\Delta t^2}{2}\int_\Gamma\left(a_{irq}a_{jqs}-\frac{c_{ijrs}}{\Delta t}\right)\overset{*}{\Phi}_\alpha\Delta U_{s,j}^{n+1}n_i\,d\Gamma$$
$$\overline{N}_{\alpha r}^n=-\int_\Gamma\left[\Delta t\overset{*}{\Phi}_\alpha\left(F_{ir}^n+G_{ir}^n\right)-\frac{\Delta t^2}{2}a_{irs}\overset{*}{\Phi}_\alpha F_{js,j}^n\right]n_i\,d\Gamma$$

It is interesting to note that both (13.2.8) and (13.2.16) are identical if the first integral of $B_{\alpha\beta rs}$ in (13.2.8) is negligible or $\mathbf{e}_i=\mathbf{b}_i-\frac{\partial\mathbf{c}_{ij}}{\partial x_j}\cong 0$, in which the role of the diffusion Jacobian $\mathbf{b}_i$ no longer exists. However, in other formulations such as in FDV (see Section 6.5 and Section 13.6), the diffusion Jacobian is shown to be important in modeling convection-diffusion interactions.

13.2.2 TAYLOR-GALERKIN METHODS WITH OPERATOR SPLITTING

If the source term $\mathbf{B}$ contains time scales widely disparate in comparison with fluid convection time scales such as occur in chemical reactions, then it is advantageous to split the Navier-Stokes system of equations into two parts so that the flow can be treated explicitly whereas the source terms are accommodated implicitly, a scheme known as the point implicit method. To this end, we may split the governing equations (13.1.7) into two parts:

$$\frac{\partial\mathbf{U}}{\partial t}+\frac{\partial\mathbf{F}_i}{\partial x_i}+\frac{\partial\mathbf{G}_i}{\partial x_i}=\mathbf{0}$$
$$\frac{\partial\mathbf{U}}{\partial t}=\mathbf{B} \tag{13.2.17a,b}$$

where (13.2.17) is identified as the fluid operator written in two-step Taylor-Galerkin method.

Step 1

$$\Delta \mathbf{U}^{n+1/2} = \mathbf{U}^{n+1/2} - \mathbf{U}^{n} = -\frac{\Delta t}{2}\left(\frac{\partial \mathbf{F}_i}{\partial x_i} + \frac{\partial \mathbf{G}_i}{\partial x_i}\right)^{n}, \quad A_{\alpha\beta}\delta_{rs}U_{\beta s}^{n+1/2} = Q_{\alpha r}^{n} \tag{13.2.18a}$$

Step 2

$$\Delta \mathbf{U}^{n+1} = -\Delta t\left(\frac{\partial \mathbf{F}_i}{\partial x_i} + \frac{\partial \mathbf{G}_i}{\partial x_i}\right)^{n+1/2}, \qquad A_{\alpha\beta}\delta_{rs}U_{\beta s}^{n+1} = Q_{\alpha r}^{n+1/2} \tag{13.2.18b}$$

with the right-hand side of (13.2.18a,b) consisting of domain and boundary integrals as usual.

The source term operator is provided with the intermediate iterative increment $m+1$ and m between $n+1$ and n so that

$$\frac{\partial \mathbf{U}^{m+1}}{\partial t} = \mathbf{B}^{m+1} \tag{13.2.19}$$

where

$$\frac{\partial \mathbf{U}^{m+1}}{\partial t} = \frac{\mathbf{U}^{m+1} - \mathbf{U}^{n}}{\Delta t} = \frac{\Delta \mathbf{U}^{m+1}}{\Delta t} + \frac{\Delta \mathbf{U}^{m}}{\Delta t} \tag{13.2.20a}$$

$$\mathbf{B}^{m+1} = \mathbf{B}^{m} + \frac{\partial \mathbf{B}}{\partial \mathbf{U}}\Delta \mathbf{U}^{m+1} \tag{13.2.20b}$$

with

$$\Delta \mathbf{U}^{m+1} = \mathbf{U}^{m+1} - \mathbf{U}^{m}, \qquad \Delta \mathbf{U}^{m} = \mathbf{U}^{m} - \mathbf{U}^{n}$$

Substituting (13.2.20a,b) into (13.2.19) yields

Step 3

$$\left(\mathbf{I} - \Delta t\frac{\partial \mathbf{B}}{\partial \mathbf{U}}\right)\Delta \mathbf{U}^{m+1} = -\Delta \mathbf{U}^{m} + \Delta t\mathbf{B}^{m} \tag{13.2.21}$$

To implement these three steps, we must first obtain the finite element analogs (13.2.18a,b) using the standard approach. The Galerkin finite element formulation of (13.2.21) gives

$$(A_{\alpha\beta}\delta_{rs} - \Delta t\, B_{\alpha\beta rs})\,\Delta \mathbf{U}_{\beta s}^{m+1} = -A_{\alpha\beta}\delta_{rs}\Delta \mathbf{U}_{\beta s}^{m} + \Delta t\; A_{\alpha\beta}\delta_{rs}\mathbf{B}_{\beta s}^{m} \tag{13.2.22}$$

with

$$A_{\alpha\beta} = \int_{\Omega} \Phi_{\alpha}\Phi_{\beta}\, d\Omega \tag{13.2.23a}$$

$$B_{\alpha\beta rs} = \int_{\Omega} f_{rs}\Phi_{\alpha}\Phi_{\beta}\, d\Omega \tag{13.2.23b}$$

$$f_{rs} = \frac{\partial \mathbf{B}_{(r)}}{\partial \mathbf{U}_{(s)}} \tag{13.2.23c}$$

Here, ΔU^m is set equal to ΔU^{n+1} with the final solution being ΔU^{m+1}. The solution will begin with the initial and boundary conditions, followed by steps 1, 2, and 3 being repeated until convergence. Applications of this scheme are demonstrated in Section 22.6.1.

13.2.3 GENERALIZED GALERKIN METHODS

Recall that, in Section 11.2, TGM is shown to be a special case of generalized Galerkin methods (GGM) in dealing with the linearized Burgers' equations. Such is not the case for the Navier-Stokes system of equations, as demonstrated by the nonlinear Burgers' equations in Section 11.2.5.

Constructing the double projections of the residual of the Navier-Stokes system of equations in terms of Jacobians onto the spatial and temporal test functions, we obtain

$$(\hat{W}(\xi), (\Phi_\alpha, \mathbf{R})) = \int_\xi \hat{W}(\xi) \int_\Omega \Phi_\alpha \left(\frac{\partial \mathbf{U}}{\partial t} + \mathbf{a}_i \frac{\partial \mathbf{U}}{\partial x_i} + \mathbf{b}_i \frac{\partial \mathbf{U}}{\partial x_i} + \mathbf{c}_{ij} \frac{\partial^2 \mathbf{U}}{\partial x_i \partial x_j} - \mathbf{B} \right) d\Omega d\xi = 0 \tag{13.2.24}$$

or without the Jacobians,

$$(\hat{W}(\xi), (\Phi_\alpha, \mathbf{R})) = \int_\xi \hat{W}(\xi) \int_\Omega \Phi_\alpha \left(\frac{\partial \mathbf{U}}{\partial t} + \frac{\partial \mathbf{F}_i}{\partial x_i} + \frac{\partial \mathbf{G}_i}{\partial x_i} - \mathbf{B} \right) d\Omega d\xi = 0 \tag{13.2.25}$$

Using the various forms of the temporal test functions $W(\xi)$ and temporal parameters η as given in Chapter 10, we obtain numerous options for the finite element equations from (13.2.24) or from (13.2.25).

For simplicity, let us examine (13.2.24), using the temporal test function, $W(\xi) = \delta(\xi - \frac{1}{2})$ or $W(\xi) = 1$ with linear variations of nodal values of the conservation variables. The generalized Galerkin finite element equations are of the form

$$\left(A_{\alpha\beta}\delta_{rs} + \frac{\Delta t}{2}(B_{\alpha\beta rs} + K_{\alpha\beta rs}) \right) \Delta U_{\beta s}^{n+1} = H_{\alpha r}^n + N_{\alpha r}^n \tag{13.2.26}$$

where

$$A_{\alpha\beta} = \int_\Omega \Phi_\alpha \Phi_\beta d\Omega \qquad B_{\alpha\beta rs} = -\int_\Omega (a_{irs} + b_{irs}) \Phi_{\alpha,i} \Phi_\beta d\Omega$$

$$K_{\alpha\beta rs} = \int_\Omega c_{ijrs} \Phi_{\alpha,i} \Phi_{\beta,j} d\Omega \qquad H_{\alpha r}^n = \Delta t \int_\Omega \Phi_\alpha \Phi_\beta B_{\beta r} d\Omega$$

$$N_{\alpha r}^n = \Delta t \int_\Gamma \overset{*}{\Phi}_\alpha \left(F_{ir}^n + G_{ir}^n \right) n_i \, d\Gamma$$

Similarly, for (13.2.25), we obtain

$$A_{\alpha\beta}\delta_{rs}\Delta U_{\beta s}^{n+1} = \frac{\Delta t}{2}\left[E_{\alpha\beta i}\left(F_{\beta ir}^n + G_{\beta ir}^n \right) \right] + \Delta t \left(H_{\alpha r}^n + N_{\alpha r}^n \right) \tag{13.2.27}$$

where

$$E_{\alpha\beta i} = \int_\Omega \Phi_{\alpha,i} \Phi_\beta \, d\Omega$$

with all other notations being the same as in (13.2.26).

For the solution of (13.2.27), we may begin with the fractional step $n+1/2$ in an explicit scheme, which is updated in the following step, $n+1$.

Step 1

$$A_{\alpha\beta}\delta_{rs}\Delta U_{\beta s}^{n+1/2} = \frac{\Delta t}{2}\left[E_{\alpha\beta i}\left(F_{\beta ir}^{n} + G_{\beta ir}^{n}\right)\right] + 2\left(H_{\alpha r}^{n} + N_{\alpha r}^{n}\right) \tag{13.2.28}$$

Step 2

$$A_{\alpha\beta}\delta_{rs}\Delta U_{\beta s}^{n+1} = \frac{\Delta t}{2}\left[E_{\alpha\beta i}\left(F_{\beta ir}^{n+\frac{1}{2}} + G_{\beta ir}^{n+\frac{1}{2}}\right)\right] + 2\left(H_{\alpha r}^{n+\frac{1}{2}} + N_{\alpha r}^{n}\right) \tag{13.2.29}$$

The nodal values, $F_{\beta ir}^{n+1/2}$, $G_{\beta ir}^{n+1/2}$, and $H_{\alpha r}^{n+1/2}$ at step 1, are estimated or determined from the boundary conditions, and $F_{\beta ir}^{n+1}$, $G_{\beta i}^{n+1}$, and $H_{\alpha r}^{n+1}$ at step 2 are calculated from $U_{\beta s}^{n+\frac{1}{2}}$ of step 1.

As was demonstrated in (11.2.12), it is necessary to add the numerical diffusion integral (13.2.9) to the convection matrix in (13.2.26) for high-speed convection-dominated flows.

13.3 GENERALIZED PETROV-GALERKIN METHODS

13.3.1 NAVIER-STOKES SYSTEM OF EQUATIONS IN VARIOUS VARIABLE FORMS

In Chapter 11, we studied the generalized Petrov-Galerkin (GPG) methods, also known as the streamline upwind Petrov-Galerkin (SUPG) methods, streamline diffusion methods (SDM), or Galerkin/least squares (GLS) as discussed in Sections 11.2 and 11.3. They were originally developed for incompressible flows, and subsequently extended to compressible flows governed by the Navier-Stokes system of equations. These methods were explored extensively by Hughes and others and are now considered as some of the most robust computational schemes that deal with discontinuities such as in shock waves. In Sections 11.3 and 11.4, it was suggested that SUPG, SDM, and GLS be called GPG for the sake of uniformity and convenience. This is because all of these methods provide numerical diffusion test functions of various forms in addition to the standard Galerkin test functions, leading to the Petrov-Galerkin methods. The concept of space/time approximations suggests and lends itself to the generalized Petrov-Galerkin (GPG) methods.

As demonstrated in Sections 11.3 and 11.4, the basic idea is to apply numerical diffusion in the direction of the streamline parallel to the velocity as in (11.3.29). Sharp discontinuities require additional numerical diffusion parallel to the velocity gradients directed toward the acceleration as in (11.3.35b), known as the discontinuity-capturing scheme. These treatments were developed for Burgers' equations where the velocity can be identified as a single variable.

In dealing with multivariables such as in the Navier-Stokes system of equations, however, numerical diffusion test functions are modified accordingly. To this end, let us consider the conservation form of the Navier-Stokes system of equations,

$$\mathbf{R} = \frac{\partial \mathbf{U}}{\partial t} + \frac{\partial \mathbf{F}_i}{\partial x_i} + \frac{\partial \mathbf{G}_i}{\partial x_i} - \mathbf{B} = 0 \tag{13.3.1a}$$

or

$$\mathbf{R} = \frac{\partial \mathbf{U}}{\partial t} + (\mathbf{a}_i + \mathbf{b}_i)\frac{\partial \mathbf{U}}{\partial x_i} + \mathbf{c}_{ij}\frac{\partial^2 \mathbf{U}}{\partial x_i \partial x_j} - \mathbf{B} = 0 \tag{13.3.1b}$$

where $\mathbf{a}_i$, $\mathbf{b}_i$, and $\mathbf{c}_{ij}$ denote the Jacobians of convection, diffusion, and diffusion gradients, respectively, as shown in Section 13.2. It should be noted that, in some applications in CFD, the diffusion Jacobian $\mathbf{b}_i$ is neglected, but it is important where inviscid-viscous interactions are taken into account such as in FDV to be discussed in Section 13.6.

Although the governing equations given by either (13.3.1a) or (13.3.1b) may be solved using the GPG methods, it is possible that improved solutions are obtained if the conservation variables are transformed into entropy variables in which the Clausius-Duhem inequality is satisfied, contributing to numerical stability [Harten, 1983; Tadmor, 1984; Hughes, Franca, and Mallet, 1986; Hauke and Hughes, 1998].

The relationship between conservation variables U and entropy variables V can be established using the following definitions:

Conservation Variables

$$\mathbf{U} = \begin{bmatrix} U_1 \\ U_2 \\ U_3 \\ U_4 \\ U_5 \end{bmatrix} = \begin{bmatrix} \rho \\ \rho \mathrm{v}_1 \\ \rho \mathrm{v}_2 \\ \rho \mathrm{v}_3 \\ \rho E \end{bmatrix} = \rho\varepsilon \begin{bmatrix} -V_5 \\ V_2 \\ V_3 \\ V_4 \\ 1 - \dfrac{V_2^2 + V_3^2 + V_4^2}{2V_5} \end{bmatrix} \tag{13.3.2}$$

Entropy Variables

$$\mathbf{V} = \begin{bmatrix} V_1 \\ V_2 \\ V_3 \\ V_4 \\ V_5 \end{bmatrix} = \frac{1}{\rho\varepsilon} \begin{bmatrix} -U_5 + \rho\varepsilon(\gamma + 1 - s) \\ U_2 \\ U_3 \\ U_4 \\ -U_1 \end{bmatrix} = \frac{1}{c_\mathrm{v} T} \begin{bmatrix} H - c_\mathrm{v} T s - \dfrac{1}{2}\mathrm{v_i v_i} \\ \mathrm{v}_1 \\ \mathrm{v}_2 \\ \mathrm{v}_3 \\ -1 \end{bmatrix} \tag{13.3.3}$$

where H is the enthalpy and s is the dimensionless entropy

$$s = \gamma - V_1 + \left(V_2^2 + V_3^2 + V_4^2\right)/2V_5 \tag{13.3.4a}$$

with

$$\rho\varepsilon = U_5 - \left(U_2^2 + U_3^2 + U_4^2\right)/2U_1 \tag{13.3.4b}$$

Substituting (13.3.2) and (13.3.3) into (13.3.1) leads to

$$\mathbf{R} = \mathbf{C}\frac{\partial \mathbf{V}}{\partial t} + \mathbf{C}_i \frac{\partial \mathbf{V}}{\partial x_i} + \mathbf{C}_{ij}\frac{\partial^2 \mathbf{V}}{\partial x_i \partial x_j} - \mathbf{B} = 0 \tag{13.3.5}$$

where the entropy variable Jacobians are defined as

$$\mathbf{C} = \frac{\partial \mathbf{U}}{\partial \mathbf{V}}, \qquad \mathbf{C}_i = (\mathbf{a}_i + \mathbf{b}_i)\mathbf{C}, \qquad \mathbf{C}_{ij} = \mathbf{c}_{ij}\mathbf{C} \tag{13.3.6a,b,c}$$

with the explicit form of the entropy variable Jacobian $\mathbf{C}$ being given in terms of the entropy variables as follows [Shakib, Hughes, and Johan, 1991]:

$$\mathbf{C} = \frac{\rho\varepsilon}{\bar{\gamma} V_5} \begin{bmatrix} -V_5^2 & e_1 & e_2 & e_3 & V_5(1-k_1) \\ & c_1 & d_1 & d_2 & V_2 k_2 \\ & & c_2 & d_3 & V_3 k_2 \\ & & & c_3 & V_4 k_2 \\ symm. & & & & -k_3 \end{bmatrix} \tag{13.3.7}$$

with

$$\begin{aligned} \overline{\gamma} &= \gamma - 1 \\ k_1 &= \frac{1}{2}\left(V_2^2 + V_3^2 + V_4^2\right)/V_5 \\ k_2 &= k_1 - \gamma \\ k_3 &= k_1^2 - 2\gamma k_1 + \gamma \\ k_4 &= k_2 - \gamma \\ k_5 &= k_2^2 - \overline{\gamma}(k_1 + k_2) \end{aligned} \qquad \begin{aligned} c_1 &= \overline{\gamma} V_5 - V_2^2 \\ c_2 &= \overline{\gamma} V_5 - V_3^2 \\ c_3 &= \overline{\gamma} V_5 - V_4^2 \\ d_1 &= -V_2 V_3 \\ d_2 &= -V_2 V_4 \\ d_3 &= -V_3 V_4 \end{aligned} \qquad \begin{aligned} e_1 &= V_2 V_5 \\ e_2 &= V_3 V_5 \\ e_3 &= V_4 V_5 \end{aligned}$$

It should be noted that all coefficient matrices, $\mathbf{C}$, $\mathbf{C}_i$, and $\mathbf{C}_{ij}$ are symmetric, and the eigenvalues associated with the convective terms are well conditioned.

Primitive Variables

For calculations involving both compressible and incompressible flows, the formulations based on conservation variables may lead to difficulties when the incompressible limit ($M_\infty = 0$) is approached. In this case, convergence toward a steady state can be very slow. To circumvent such difficulties, the concept of preconditioning is introduced as in FDM [Choi and Merkle, 1993] and also as in FEM [Hauke and Hughes, 1998] by means of the primitive variable Jacobian,

$$\mathbf{D} = \frac{\partial \mathbf{U}}{\partial \mathbf{W}} \tag{13.3.8}$$

where $\mathbf{W}$ represents the primitive variables,

$$\mathbf{W} = \begin{bmatrix} \rho \\ v_1 \\ v_2 \\ v_3 \\ T \end{bmatrix} \tag{13.3.9}$$

Introducing (13.3.8) and (13.3.9) into (13.3.1), we obtain

$$\mathbf{R} = \mathbf{D}\frac{\partial \mathbf{W}}{\partial t} + \mathbf{D}_i \frac{\partial \mathbf{W}}{\partial x_i} + \mathbf{D}_{ij} \frac{\partial^2 \mathbf{W}}{\partial x_i \partial x_j} - \mathbf{B} = 0 \tag{13.3.10}$$

with

$$\mathbf{D}_i = (\mathbf{a}_i + \mathbf{b}_i)\mathbf{D} \tag{13.3.11}$$

$$\mathbf{D}_{ij} = \mathbf{c}_{ij}\mathbf{D} \tag{13.3.12}$$

where the explicit form of the primitive variable Jacobian D is given below,

$$\mathbf{D} = \begin{bmatrix} 1 & 0 & 0 & 0 & 0 \\ \mathrm{v}_1 & \rho & 0 & 0 & 0 \\ \mathrm{v}_2 & 0 & \rho & 0 & 0 \\ \mathrm{v}_3 & 0 & 0 & \rho & 0 \\ \hat{\varepsilon} & \rho\mathrm{v}_1 & \rho\mathrm{v}_2 & \rho\mathrm{v}_3 & \rho\mathrm{c}_\mathrm{v} \end{bmatrix} \tag{13.3.13}$$

with

$$\hat{\varepsilon} = c_p T + \frac{1}{2}\mathrm{v_i v_i} - c_\mathrm{v} T(\gamma - 1)$$

The governing equations given by (13.3.10) are well behaved as the eigenvalues of the convective terms are well conditioned even when the incompressible limit is reached.

13.3.2 THE GPG WITH CONSERVATION VARIABLES

Following the procedure presented in Section 11.4, let us now consider the GPG formulations of the Navier-Stokes system of equations in terms of conservation variables given by (13.3.1).

$$\int_\xi \hat{W}(\xi) \int_\Omega \left[(\Phi_\alpha + \Psi_\alpha^{(a)}) \left(\frac{\partial \mathbf{U}}{\partial t} + (\mathbf{a}_i + \mathbf{b}_i)\frac{\partial \mathbf{U}}{\partial x_i} + \mathbf{c}_{ij}\frac{\partial^2 \mathbf{U}}{\partial x_i \partial x_j} - \mathbf{B} \right) + \Psi^{(b)} \mathbf{a}_i \frac{\partial \mathbf{U}}{\partial x_i} \right] d\Omega d\xi = 0 \tag{13.3.14}$$

As shown earlier in Section 11.4, the integration by parts is to be performed only to those terms associated with the Galerkin test function Φ_α. With assumptions made similarly as in the case of the Burgers equation for those terms associated with the numerical diffusion test function for streamline diffusion, we obtain

$$\int_\xi \hat{W}(\xi) \left[\int_\Omega \left\{ \Phi_\alpha \left(\frac{\partial \mathbf{U}}{\partial t} - \mathbf{B} \right) - (\Phi_{\alpha,i}(\mathbf{a}_i + \mathbf{b}_i)\mathbf{U} + \Phi_{\alpha,i}\mathbf{c}_{ij}\mathbf{U}_{,j}) \right\} d\Omega + \int_\Gamma \overset{*}{\Phi}_\alpha (\mathbf{F}_i + \mathbf{G}_i) n_i d\Gamma \right] d\xi + \int_\xi \hat{W}(\xi) \int_\Omega \left[\Psi_\alpha^{(a)} (\mathbf{a}_i \mathbf{U}_{,i} + \mathbf{c}_{ij}\mathbf{U}_{,ji}) + \Psi_\alpha^{(b)} \mathbf{a}_i \mathbf{U}_{,i} \right] d\Omega d\xi = 0 \tag{13.3.15}$$

where the numerical diffusion test functions are given by

$$\Psi_\alpha^{(a)} = \tau \mathbf{a}_i \Phi_{\alpha,i}, \qquad \text{streamline diffusion in GPG} \tag{13.3.16a}$$

$$\Psi_\alpha^{(a)} = \tau \mathbf{L}\Phi_\alpha, \qquad \text{streamline diffusion in GLS} \tag{13.3.16b}$$

$$\Psi_\alpha^{(b)} = \tau^{(b)} \mathbf{a}_i \Phi_{\alpha,i}, \qquad \text{discontinuity-capturing} \tag{13.3.17}$$

The differential operator L in (13.3.16b) is written as

$$\mathbf{L} = \frac{\partial}{\partial t} + \mathbf{a}_i \frac{\partial}{\partial x_i} + \mathbf{c}_{ij} \frac{\partial^2}{\partial x_i \partial x_j} \tag{13.3.18}$$

With the trial functions applied to the conservation variables, together with linear temporal test functions (Section 10.2), we arrive at

$$\begin{aligned}
&[A_{\alpha\beta rs} + \eta\Delta t(C_{\alpha\beta rs} + D_{\alpha\beta rs} - B_{\alpha\beta rs} - K_{\alpha\beta rs})]U_{\beta s}^{n+1}\Delta t \\
&\quad = [A_{\alpha\beta rs} - (1-\eta)(C_{\alpha\beta rs} + D_{\alpha\beta rs} - B_{\alpha\beta rs} - K_{\alpha\beta rs})]U_{\beta s}^{n} \\
&\qquad + \Delta t\left(H_{\alpha r}^{n} + N_{\alpha r}^{n}\right)
\end{aligned} \tag{13.3.19}$$

with

$$A_{\alpha\beta rs} = \int_\Omega \delta_{rs}\Phi_\alpha\Phi_\beta d\Omega \tag{13.3.20a}$$

$$C_{\alpha\beta rs} = \int_\Omega (\overline{\tau}a_{irt}a_{jts} + \overline{\upsilon}\delta_{ij}\delta_{rs})\Phi_{\alpha,i}\Phi_{\beta,j}d\Omega \tag{13.3.20b}$$

$$K_{\alpha\beta rs} = \int_\Omega c_{ijrs}\Phi_{\alpha,i}\Phi_{\beta,j}d\Omega \tag{13.3.20c}$$

$$B_{\alpha\beta rs} = \int_\Omega (a_{irs} + b_{irs})\Phi_{\alpha,i}\Phi_\beta d\Omega \tag{13.3.20d}$$

$$D_{\alpha\beta rs} = \int_\Omega \overline{\tau}a_k c_{ijrs}\Phi_{\alpha,k}\Phi_{\beta,ji}d\Omega \tag{13.3.20e}$$

$$H_{\alpha r}^{n} = \int_\Omega \Phi_\alpha B_r d\Omega \tag{13.3.20f}$$

$$N_{\alpha r}^{n} = \int_\Gamma \overset{*}{\Phi}_\alpha(F_{ir} + G_{ir})n_i d\Gamma \tag{13.3.20g}$$

where the intrinsic time scale $\overline{\tau}$ and the discontinuity-capturing factor $\overline{\upsilon}$ constitute the equivalent artificial diffusivity,

$$\overline{\tau} = \left(g^{ij}a_{irt}a_{jst}C_{rs}^{-1}\right)^{-\frac{1}{2}} \tag{13.3.21}$$

$$\overline{\upsilon} = \max(0, \overline{\upsilon}_d - \overline{\upsilon}_s) \tag{13.3.22}$$

with

$$\overline{\upsilon}_d = \left(\frac{C_{rs}^{-1}a_{itr}a_{jus}U_{t,i}U_{u,j}}{C_{vw}g^{mn}U_{v,m}U_{w,n}}\right)^{\frac{1}{2}}$$

$$\overline{\upsilon}_s = \frac{\overline{\tau}a_{irt}a_{jst}U_{r,i}U_{s,j}}{C_{uv}U_{u,k}U_{v,k}}$$

where C_{rs} is the entropy variable Jacobian (13.3.5) and g^{mn} is the contravariant metric tensor in the curvilinear isoparametric coordinates (Figure 11.3.3),

$$g^{mn} = \frac{\partial\xi_m}{\partial x_p}\frac{\partial\xi_n}{\partial x_p}$$

Here, the indicies i, j, k, m, n, p refer to the spatial coordinates (1,2,3) and r, s, t, ν, ν, w

denote the equation number (1,2,3,4,5) in the Navier-Stokes system of equations. It should be noted that the criterion used in (13.3.21) is motivated by the fact that the gradients of all variables are involved in determining the dimensionally equivalent artificial diffusivity rather than artificial time scale associated with only the velocity and velocity gradients. This is in contrast to the case of the numerical diffusion test functions developed for the Burgers' equations as given by (11.3.35b) and (11.3.38). Note also that another criterion in (13.3.22) is to ensure positive numerical diffusion for highly distorted elements.

There are other versions of numerical diffusion factors, as proposed in Hauke and Hughes [1998], Aliabadi and Tezduyar [1993], and other related references for the past decade. The basic idea is to apply the numerical diffusion in the direction of velocity for streamline diffusion and in the direction of gradients for discontinuity-capturing, as described in Section 11.3.

Instead of using the linear temporal variations, we may enhance temporal approximations with a second order accuracy of the form

$$\frac{\partial \mathbf{U}}{\partial t} = \frac{3\mathbf{U}^{n+1} - 4\mathbf{U}^{n} + \mathbf{U}^{n-1}}{2\Delta t} \tag{13.3.23}$$

together with quadratic variations of $\mathbf{U}_\beta$ between nodes,

$$\mathbf{U}_\beta = \frac{5}{8}\mathbf{U}_\beta^{n+1} + \frac{3}{4}\mathbf{U}_\beta^{n} - \frac{3}{8}\mathbf{U}_\beta^{n-1} \tag{13.3.24}$$

These approximations lead to

$$\begin{aligned}\left[3A_{\alpha\beta rs} + \frac{5}{4}\Delta t(C_{\alpha\beta rs} - K_{\alpha\beta rs})\right]\mathbf{U}_{\beta s}^{n+1} = {} & \left[4A_{\alpha\beta rs} - \frac{3}{2}\Delta t(B_{\alpha\beta rs} - D_{\alpha\beta rs})\right]\mathbf{U}_{\beta s}^{n} \\ & - \left[A_{\alpha\beta rs} - \frac{3}{4}\Delta t(B_{\alpha\beta rs} - D_{\alpha\beta rs})\right]\mathbf{U}_{\beta s}^{n-1} \\ & + \Delta t\left(H_{\alpha r}^{n} + N_{\alpha r}^{n}\right)\end{aligned} \tag{13.3.25}$$

Other possibilities for temporal approximations such as discussed in Section 10.2 may be considered for applications to various physical problems as required for higher order accuracy.

13.3.3 THE GPG WITH ENTROPY VARIABLES

The GPG formulations in terms of entropy variables can be carried out similarly as in (13.3.14) using (13.3.5),

$$\begin{aligned}\int_\Omega \hat{W}(\xi)\int_\Omega \Bigg[\left(\Phi_\alpha + \Psi_\alpha^{(a)}\right)\left(\mathbf{C}\frac{\partial \mathbf{V}}{\partial t} + \mathbf{C}_i\frac{\partial \mathbf{V}}{\partial x_i} + \mathbf{C}_{ij}\frac{\partial^2 \mathbf{V}}{\partial x_i \partial x_j} - \mathbf{B}\right) \\ + \Psi_\alpha^{(b)}\mathbf{a}_i\mathbf{C}\frac{\partial \mathbf{V}}{\partial x_i}\Bigg] d\Omega d\xi = 0\end{aligned} \tag{13.3.26}$$

which leads to

$$\begin{aligned}&[A_{\alpha\beta rs} + \eta\Delta t(C_{\alpha\beta rs} + D_{\alpha\beta rs} - B_{\alpha\beta rs} - K_{\alpha\beta rs})]V_{\beta s}^{n+1} \\ &\quad = [A_{\alpha\beta rs} - (1-\eta)\Delta t(C_{\alpha\beta rs} + D_{\alpha\beta rs} - B_{\alpha\beta rs} - K_{\alpha\beta rs})]V_{\beta s}^{n} \\ &\qquad + \Delta t\left(H_{\alpha r}^{n} + N_{\alpha r}^{n}\right)\end{aligned} \tag{13.3.27}$$

where

$$A_{\alpha\beta rs} = \int_\Omega C_{rs}\Phi_\alpha\Phi_\beta d\Omega$$

$$C_{\alpha\beta rs} = \int_\Omega (\overline{\tau}a_{irt}a_{jst} + \overline{\nu}_{rs}\delta_{ij})\Phi_{\alpha,i}\Phi_{\beta,j}d\Omega$$

$$K_{\alpha\beta rs} = \int_\Omega c_{ijrt}C_{st}\Phi_{\alpha,i}\Phi_{\beta,j}d\Omega$$

$$B_{\alpha\beta rs} = \int_\Omega a_{irt}C_{st}\Phi_{\alpha,i}\Phi_\beta d\Omega$$

$$D_{\alpha\beta rs} = \int_\Omega \overline{\tau}a_k c_{ijrt}C_{st}\Phi_{\alpha,k}\Phi_{\beta,ij}d\Omega$$

$$H^n_{\alpha r} = \int_\Omega \Phi_\alpha B_r d\Omega$$

$$N^n_{\alpha r} = -\int_\Gamma \overset{*}{\Phi}_\alpha (F_{ir} + G_{ir})n_i d\Gamma$$

with

$$\overline{\tau} = \left(g^{ij}C_{irt}C_{jst}C^{-1}_{rs}\right)^{-\frac{1}{2}} \tag{13.3.28}$$

$$\overline{\upsilon}_{rs} = \max(0, \overline{\upsilon}_d - \overline{\upsilon}_s)C_{rs} \tag{13.3.29}$$

$$\overline{\upsilon}_d = \left(\frac{C^{-1}_{rs}C_{itr}C_{jus}V_{t,i}V_{u,j}}{C_{vw}g^{mn}V_{v,m}V_{w,n}}\right)^{\frac{1}{2}}$$

$$\overline{\upsilon}_s = \frac{\overline{\tau}C_{irt}C_{jst}V_{r,i}V_{s,j}}{C_{rs}V_{r,k}V_{s,k}}$$

The criterion given in (13.3.29) is to ensure that the discontinuity-capturing diffusivity is larger than the streamline diffusivity, which may not be true for highly distorted elements. As in the case of conservation variables, temporal approximations may be enhanced with a second order accuracy as in (13.3.22). Further details of the GPG with entropy variables are found in Hughes et al. [1986], Shakib et al. [1991], and Hauke and Hughes [1998].

13.3.4 THE GPG WITH PRIMITIVE VARIABLES

The projections of the residuals of the governing equations in terms of primitive variables (13.3.10) onto the various test functions are given by

$$\int_\xi \hat{W}(\xi)\int_\Omega \left[\left(\Phi_\alpha + \Psi^{(a)}_\alpha\right)\left(\mathbf{D}\frac{\partial W}{\partial t} + \mathbf{D}_i\frac{\partial W}{\partial x_i} + \mathbf{D}_{ij}\frac{\partial^2 W}{\partial x_i \partial x_j} - \mathbf{B}\right)\right.$$
$$\left. + \Psi^{(b)}_\alpha \mathbf{a}_i \mathbf{D}\frac{\partial \mathbf{W}}{\partial x_i}\right]d\Omega d\xi = 0 \tag{13.3.30}$$

The resulting algebraic equations are of the form

$$[A_{\alpha\beta rs} + \eta\Delta t(C_{\alpha\beta rs} - K_{\alpha\beta rs})]W^{n+1}_{\beta s}$$
$$= [A_{\alpha\beta rs} - (1-\eta)\Delta t(B_{\alpha\beta rs} + D_{\alpha\beta rs})]W^{n}_{\beta s} + \Delta t\left(H^n_{\alpha r} + N^n_{\alpha r}\right) \tag{13.3.31}$$

where

$$A_{\alpha\beta rs} = \int_\Omega D_{rs}\Phi_\alpha\Phi_\beta d\Omega$$

$$C_{\alpha\beta rs} = \int_\Omega (\overline{\tau}a_{irt}a_{jts} + \overline{\upsilon}_{rs}\delta_{ij})\Phi_{\alpha,i}\Phi_{\beta,j}d\Omega$$

$$K_{\alpha\beta rs} = \int_\Omega c_{ijrt}D_{ts}\Phi_{\alpha,i}\Phi_{\beta,i}d\Omega$$

$$B_{\alpha\beta rs} = \int_\Omega a_{irt}D_{ts}\Phi_{\alpha,i}\Phi_\beta d\Omega$$

$$D_{\alpha\beta rs} = \int_\Omega \overline{\tau}a_{krt}c_{ijtu}D_{us}\Phi_{\alpha,k}\Phi_{\beta,ji}d\Omega$$

$$H^n_{\alpha r} = \int_\Omega \Phi_\alpha B_r d\Omega$$

$$N^n_{\alpha r} = -\int_\Gamma \overset{*}{\Phi}_\alpha(F_{ir} + G_{ir})n_i d\Gamma$$

with

$$\overline{\tau} = \left(g^{ij}D_{irt}D_{jts}D^{-1}_{rs}\right)^{-\frac{1}{2}} \tag{13.3.32}$$

$$\overline{\upsilon}_{rs} = \max(0, \overline{\upsilon}_d - \overline{\upsilon}_s)D_{rs} \tag{13.3.33}$$

$$\overline{\upsilon}_d = \left(\frac{D^{-1}_{rs}D_{itr}D_{jus}W_{t,i}W_{u,j}}{D_{vw}g^{mn}W_{v,m}W_{w,n}}\right)^{\frac{1}{2}}$$

$$\overline{\upsilon}_s = \frac{\overline{\tau}D_{irt}D_{jts}W_{r,i}W_{s,j}}{D_{uv}W_{u,k}W_{v,k}}$$

Once again, the transformation of the conservation variable into primitive variables results in appropriate modifications of the parameters involved in the numerical diffusion test functions.

13.4 CHARACTERISTIC GALERKIN METHODS

The characteristic Galerkin methods (CGM) are based on the concept of trajectories or characteristics [Zienkiewicz and Codina, 1995; Zienkiewicz et al., 1998; Codina, Vazquez, and Zienkiewicz, 1998] with

$$x^n_i = x^{n+1}_i - \Delta t\mathrm{v}^n_i \tag{13.4.1}$$

Differentiating (13.4.1) with respect to time, we have

$$\mathrm{v}^n_i = \mathrm{v}^{n+1}_i - \Delta t\mathrm{v}^n_j\frac{\partial \mathrm{v}^n_i}{\partial x_j} \tag{13.4.2}$$

Combining (13.4.1) and (13.4.2) leads to

$$x_i^{n+1} - x_i^n = \Delta t \mathrm{v}_i^n - \frac{\Delta t^2}{2} \mathrm{v}_j^n \frac{\partial \mathrm{v}_i^n}{\partial x_j} \tag{13.4.3}$$

The main idea of CGM is to write the governing equations along the characteristics so that the Navier-Stokes system of equations may be recast in the form similar to (13.4.3).

$$\Delta \mathbf{U}^{n+1} = \Delta t \mathbf{R}^n - \frac{\Delta t^2}{2} \mathbf{a}_j^n \frac{\partial \mathbf{R}^n}{\partial x_j} \tag{13.4.4}$$

where $\mathbf{a}_j^n$ is the convection Jacobian, with $\mathbf{R}^n$ is the residual defined as

$$\mathbf{R}^n = -\left(\frac{\partial \mathbf{F}_i{}^n}{\partial x_i} + \frac{\partial \mathbf{G}_i^n}{\partial x_i} - \mathbf{B}^n \right)$$

Instead of solving (13.4.4) directly, the fractional step approach may be used for convenience. Here, the momentum equations are solved first without pressure, followed by the continuity equation to compute the pressure. With these results, we return to the momentum equations again to update the flowfield, before the energy equation is solved.

Momentum (initially):

$$\Delta \overline{\rho \mathrm{v}}_i^{\overline{n}} = \Delta t R_i^n - \frac{\Delta t^2}{2} \mathrm{v}_k \frac{\partial \hat{R}_i^n}{\partial x_k} \tag{13.4.5}$$

with

$$R_i^n = -\frac{\partial}{\partial x_j} (\rho \mathrm{v}_i \mathrm{v}_j - \tau_{ij}) + \rho g_i$$

$$\hat{R}_i^n = R_i^n - \frac{\partial p^n}{\partial x_i}$$

Continuity:

$$\Delta \rho^n = -\Delta t \frac{\partial}{\partial x_i} \left(\rho \mathrm{v}_i^n + \theta_1 \Delta \overline{\rho \mathrm{v}}_i^{\overline{n}} \right) + \theta_1 \Delta t^2 \frac{\partial^2 p^{n+\theta_2}}{\partial x_i \partial x_i} \tag{13.4.6}$$

with

$0 \leq \theta_1, \theta_2 \leq 1$

Momentum (updated):

$$\Delta \rho \mathrm{v}_i^n = \Delta \overline{\rho \mathrm{v}}_i^{\overline{n}} - \Delta t \frac{\partial p^{n+\theta_2}}{\partial x_i} \tag{13.4.7}$$

Energy:

$$\Delta \rho E^n = \Delta t R^n - \frac{\Delta t^2}{2} \mathrm{v}_k \frac{\partial R^n}{\partial x_k} \tag{13.4.8}$$

with

$$R^n = -\frac{\partial}{\partial x_i}\left[(\rho E + p)\mathrm{v}_i - k\frac{\partial T}{\partial x_i} - \tau_{ij}\mathrm{v}_j\right]$$

The standard Galerkin approximations can now be applied to these equations separately and the solution proceeds as follows:

(1) Solve the momentum equations (13.4.5).
(2) Solve the continuity equation (13.4.6), using the mass flux obtained from step 1 to calculate the pressure.
(3) Update the mass flux with (13.4.7), using the pressure from step 2.
(4) Solve the energy equation (13.4.8) to obtain the total energy or temperature using the results obtained from step 3.
(5) Repeat the steps 1 through 4 until the steady state is reached.

To explore the physical significance of the CGM procedure, let us substitute (13.4.5) into (13.4.7) to obtain

$$\frac{\partial}{\partial t}(\rho \mathrm{v}_i) + (\rho \mathrm{v}_i \mathrm{v}_j)_{,j} + p_{,i} - \tau_{ij,j} - \rho f_i = S_i(m) \tag{13.4.9}$$

with

$$S_i(m) = \frac{\Delta t}{2}\{\mathrm{v}_k[(\rho \mathrm{v}_i \mathrm{v}_j)_{,j} + p_{,i} - \tau_{ij,j} - \rho f_i]\}_{,k} \tag{13.4.10}$$

Similarly, the continuity equation (13.4.6) and energy equation (13.4.8) are rewritten, respectively, as

$$\frac{\partial \rho}{\partial t} + (\rho \mathrm{v}_i)_{,i} = S(c) \tag{13.4.11}$$

with

$$S(c) = \frac{\Delta t}{2}[(\rho \mathrm{v}_i \mathrm{v}_j - \tau_{ij})_{,ji} + p_{,ii} - (\rho f_i)_{,i}] \tag{13.4.12}$$

by setting $\theta_1 = 1/2$ and $\theta_2 = 0$ in (13.4.6), and

$$\frac{\partial \rho E}{\partial t} + [(\rho E + p)\mathrm{v}_i - kT_{,i} - \tau_{ij}\mathrm{v}_j]_{,i} = S(e) \tag{13.4.13}$$

with

$$S(e) = \frac{\Delta t}{2}\mathrm{v}_j\left[(\rho E \mathrm{v}_i + p\mathrm{v}_i - kT_{,i} - \tau_{ik}\mathrm{v}_k)_{,i}\right]_{,j} \tag{13.4.14}$$

The consequence of the CGM process is that additional terms $S(m)$, $S(c)$, and $S(e)$ on the right-hand side of momentum, continuity, and energy equations, respectively, have been generated as numerical diffusion. It is remarkable that the combination of all equations, (13.4.5) through (13.4.8), which represents (13.4.4) can be identified in the TGM equations. The similar results arise in TGM with the right-hand side of (13.2.14)

revised by substituting

$$a_j \frac{\partial \Delta U^{n+1}}{\partial x_j} = \frac{\partial \Delta F_j{}^{n+1}}{\partial x_j}$$

The advantage of the fractional step approach is the fact that the continuity equation can be written in the form given by (13.4.11) in which the spatial second derivatives of pressure arise explicitly, acting as numerical diffusion. Of course, this effect is present, implicitly embedded, when the entire equations are solved simultaneously in TGM. An important conclusion here is that the CGM concept is found to be identical to TGM. It will be shown in Section 13.6.3 that these results arise as a special case of the flowfield-dependent variation methods.

Direct assessments of the fractional step approach can be made by applying the Galerkin formulation of (13.4.9) and (13.4.11) separately and combining the results in a matrix form:

$$\begin{bmatrix} K_{\alpha\beta ij} & C_{\alpha\beta i} \\ D_{\alpha\beta j} & B_{\alpha\beta} \end{bmatrix} \begin{bmatrix} \mathrm{v}_{\beta j} \\ \mathrm{p}_{\beta} \end{bmatrix} = \begin{bmatrix} E_{\alpha i} \\ F_{\alpha} \end{bmatrix} \tag{13.4.15}$$

where it can be shown that the presence of $B_{\alpha\beta}$ is due to the numerical diffusion terms characterized by $S_i(m)$ and $S(c)$ in (13.4.9) and (13.4.11), respectively. Otherwise, $B_{\alpha\beta}$ would have been zero, resulting in numerical instability. In this case, the so-called LBB restriction requires a special treatment in incompressible flow as discussed in Chapter 12. It is reminded that the simultaneous solution of all equations in terms of the conservation variables have the advantage of versatility and simplicity with all numerical diffusion terms appearing on the left-hand side rather than on the right-hand side.

13.5 DISCONTINUOUS GALERKIN METHODS OR COMBINED FEM/FDM/FVM METHODS

The basic idea of discontinuous Galerkin methods (DGM) is to combine FDM schemes with upwind finite differences into the FEM formulation such as standard Galerkin methods or Taylor-Galerkin methods. In this process, integration by parts in the FEM equations provides the boundary terms in which the convection numerical flux terms are discretized using the upwind FDM schemes via finite volume approximations. Thus, in DGM, all currently available CFD schemes are combined together, alternatively referred to as the combined FEM/FDM/FVM methods. Various authors have contributed to DGM. Among them are La Saint and Raviart [1974], Johnson and Pitkäranta [1986], Cockburn, Hou, and Shu [1990, 1997], and Oden, Babuska, and Baumann [1998].

In the DGM approach, we begin with the standard Galerkin integral,

$$\int_{\Omega} \Phi_{\alpha} \left(\frac{\partial \mathbf{U}}{\partial t} + \mathbf{F}_{i,i} + \mathbf{G}_{i,i} - \mathbf{B} \right) d\Omega = 0 \tag{13.5.1}$$

or

$$\int_{\Omega} \Phi_{\alpha} \left[\frac{\partial \mathbf{U}}{\partial t} + (\mathbf{a}_i \mathbf{U})_{,i} + (\mathbf{b}_i \mathbf{U} + \mathbf{c}_{ij} \mathbf{U}_{,j})_{,i} - \mathbf{B} \right] d\Omega = 0 \tag{13.5.2}$$

Integrating (13.5.1) or (13.5.2) by parts, we obtain

$$\int_\Omega \Phi_\alpha \frac{\partial \mathbf{U}}{\partial t} d\Omega - \int_\Omega \Phi_{\alpha,i}(\mathbf{F}_i + \mathbf{G}_i) d\Omega - \int_\Omega \Phi_\alpha \mathbf{B} d\Omega + \int_\Gamma \overset{*}{\Phi}_\alpha \mathbf{F}_i n_i d\Gamma + \int_\Gamma \overset{*}{\Phi}_\alpha (\mathbf{G}_i + \hat{\mathbf{G}}_i) n_i d\Gamma = 0 \tag{13.5.3}$$

with

$$\mathbf{F}_i = \mathbf{a}_i \mathbf{U}, \quad \mathbf{G}_i = \mathbf{b}_i \mathbf{U}, \quad \hat{\mathbf{G}}_i = \mathbf{c}_{ij} \mathbf{U}_{,i} \tag{13.5.4}$$

In a compact notation, we write (13.5.3) in the form

$$(A_{\alpha\beta} + B_{\alpha\beta}) \Delta \mathbf{U}_\beta^{n+1} = \mathbf{F}_\alpha + \mathbf{G}_\alpha + \mathbf{H}_\alpha \tag{13.5.5}$$

with

$$A_{\alpha\beta} = \int_\Omega \Phi_\alpha \Phi_\beta d\Omega \tag{13.5.6a}$$

$$B_{\alpha\beta} = \Delta t \int_\Omega ((a_i + b_i)(\Phi_{\alpha,i} \Phi_\beta - c_{ij} \Phi_{\alpha,i} \Phi_{\beta,j})) d\Omega \tag{13.5.6b}$$

$$\mathbf{F}_\alpha = \Delta t \int_\Omega \Phi_\alpha \mathbf{B} d\Omega \tag{13.5.6c}$$

$$\mathbf{G}_\alpha = -\Delta t \int_\Gamma \overset{*}{\Phi}_\alpha \mathbf{F}_i n_i d\Gamma \tag{13.5.6d}$$

$$\mathbf{H}_\alpha = -\Delta t \int_\Gamma \overset{*}{\Phi}_\alpha (\mathbf{G}_i + \hat{\mathbf{G}}_i) n_i d\Gamma \tag{13.5.6e}$$

Instead of using the standard Galerkin formulation of (13.5.1–13.5.3), we may utilize the Taylor-Galerkin methods (TGM) as described in Section 13.2. In this case, the expression given by (13.2.15) is used instead of (13.5.3).

$$\int_\Omega \Phi_\alpha \left\{ 1 - \frac{\Delta t^2}{2} \frac{\partial}{\partial x_i} \left(\mathbf{a}_i \mathbf{a}_j - \frac{\mathbf{c}_{ij}}{\Delta t} \right) \frac{\partial}{\partial x_j} \right\} \Delta \mathbf{U}^{n+1} d\Omega = \int_\Omega \Phi_\alpha \left\{ \Delta t \left(-\frac{\partial \mathbf{F}_i}{\partial x_i} - \frac{\partial \mathbf{G}_i}{\partial x_i} + \mathbf{B} \right)^n + \frac{\Delta t^2}{2} \frac{\partial}{\partial x_i} \left(\mathbf{a}_i \frac{\partial \mathbf{F}_j}{\partial x_j} \right)^n \right\} d\Omega \tag{13.5.7}$$

Note that the first integral on the right-hand side of (13.5.5), upon integration by parts, becomes identical to the form given in (13.5.3), resulting in the same boundary integrals. All quantities resulting from (13.5.5) are identical to those given in (13.5.6) except for (13.5.6b,c),

$$B_{\alpha\beta} = \frac{\Delta t^2}{2} \int_\Omega \left(\left(a_i a_j - \frac{c_{ij}}{\Delta t} \right) \Phi_{\alpha,i} \Phi_{\beta,j} \right) d\Omega \tag{13.5.8a}$$

$$\mathbf{F}_\alpha = \Delta t \int_\Omega \Phi_\alpha \mathbf{B} d\Omega - \Delta t \int_\Omega \Phi_{\alpha,i} (\mathbf{F}_i + \mathbf{G}_i) \, d\Omega \tag{13.5.8b}$$

Here, the boundary integrals (13.5.6d) for convection represent possible discontinuities characterized by the eigenvalues and eigenvectors of the convection Jacobian $\mathbf{a}_i$ in the

spirit of flux vector splitting. Similarly, the flux variables F_i may be reconstructed using the various FDM second order upwind schemes [Godunov, 1959; Harten, 1984; Roe, 1984; Osher, 1984; van Leer, 1979; etc.] or flux-corrected transport (FCT) [Boris and Book, 1976; Zalesak, 1979]. Recall that FDM schemes were presented in Chapter 6. The idea of DGM is to combine FDM into FEM. Some examples of various FDM schemes which may be combined to DGM are the flux vector splitting for the convection Jacobian and various second order upwind schemes as detailed in Section 6.2.

Some numerical applications of (13.5.5) have been reported by Baumann and Oden [1999] for the *hp* adaptive first order upwind scheme and by Atkins and Shu [1998] for the second order TVD upwind scheme, among others.

13.6 FLOWFIELD-DEPENDENT VARIATION METHODS

Recall that the flowfield-dependent variation (FDV) theory was developed in Section 6.5, in which the FDV equations were solved using FDM. The basic theory of FDV will not be repeated here. Thus, the reader should review the process of development presented in Section 6.5 thoroughly. In this section, some additional items of interest such as the source terms of gravity, surface tension, and chemical species reaction rate are included. These and other aspects of the FDV theory to be emphasized are presented next.

13.6.1 BASIC FORMULATION

As stated in Section 6.5, the FDV theory was devised in response to the need to characterize the complex physics of shock wave turbulent boundary layers in which transitions between, and interactions of, inviscid/viscous, incompressible/compressible, and laminar/turbulent flows constitute the most complex physical phenomena in fluid dynamics [Chung and his co-workers, 1996–1999]. The complexities of physics, in general, lead directly to computational difficulties. This is where the very low velocity in the vicinity of the wall and very high velocity far away from the wall coexist within a domain of study. Transitions from one type of flow to another and interactions between two distinctly different flows have been studied for many years, both experimentally and numerically. Incompressible flows were analyzed using the pressure-based formulation with the primitive variables for the implicit solution of the Navier-Stokes system of equations together with the pressure Poisson equation. On the other hand, compressible flows were analyzed using the density-based formulation with the conservation variables for the explicit solution of the Navier-Stokes system of equations.

In a given domain, however, dealing with all speed flows of various physical properties, we encounter different equations of state for compressible and incompressible flows, transitions between laminar and turbulent flows, dilatational dissipation due to compressibility as well as difficulties of satisfying the mass conservation or incompressibility condition. To cope with this situation, we must provide very special and powerful numerical treatments. The FDV scheme has been devised toward resolving these issues.

For most of the CFD methods, the numerical formulation begins with a particular physical phenomenon. Thus, if the physics is changed, then the numerics must be accordingly changed. Our goal in FDV, instead, is to derive a scheme in which all possible physical aspects are already taken into account in the final form of the governing

equations so that FDM or FEM is reduced to an option of how to discretize between nodal points or elements. Thus, the formulation of FDV procedure in terms of FEM is identical to that of FDM.

To this end, we shall consider the most general form of Navier-Stokes system of equations in conservation form, including the chemically reacting species equations and source terms for the body force, surface tension, and chemical reaction rates, which will be useful for applications of FDV to problems in Part Five.

$$\frac{\partial \mathbf{U}}{\partial t} + \frac{\partial \mathbf{F}_i}{\partial \mathbf{x}_i} + \frac{\partial \mathbf{G}_i}{\partial \mathbf{x}_i} = \mathbf{B} \tag{13.6.1}$$

where $\mathbf{U}, \mathbf{F}_i, \mathbf{G}_i$, and $\mathbf{B}$ denote the conservation flow variables, convection flux variables, diffusion flux variables, and source terms, respectively,

$$\mathbf{U} = \begin{bmatrix} \rho \\ \rho \mathrm{v}_j \\ \rho E \\ \rho Y_k \end{bmatrix}, \quad \mathbf{F}_i = \begin{bmatrix} \rho \mathrm{v}_i \\ \rho \mathrm{v}_i \mathrm{v}_j + p\delta_{ij} \\ \rho E \mathrm{v}_i + p\mathrm{v}_i \\ \rho Y_k \mathrm{v}_i \end{bmatrix}, \quad \mathbf{G}_i = \begin{bmatrix} 0 \\ -\tau_{ij} \\ -\tau_{ij}\mathrm{v}_j - kT_{,i} - \sum \rho c_{pk} T D_{km} Y_{k,i} \\ -\rho D_{km} Y_{k,i} \end{bmatrix},$$

$$\mathrm{B} = \begin{bmatrix} 0 \\ \rho f_j \\ -\sum H_k^0 \omega_k + \rho f_j \mathrm{v}_j \\ \omega_k \end{bmatrix}$$

where $f_j = \sum_{k=1}^{N} Y_k f_{kj}$ is the body force, Y_k is the chemical species, H_k^o is the zero-point enthalpy, ω_k is the reaction rate, and D_{km} is the binary diffusivity. Additional equations for vibrational and electronic energies may be included in (13.6.1) for hypersonics (see Section 22.5).

Using the Taylor series expansion of $\mathbf{U}^{n+1}$ in terms of the FDV parameters, following the process given by (6.5.2) through (6.5.13a,b) together with the source terms, the residual of the Navier-Stokes system of equations can be written as

$$\begin{aligned} \mathbf{R} = \Delta \mathbf{U}^{n+1} - \Delta t \Bigg[& -\frac{\partial \mathbf{F}_i^n}{\partial x_i} - \frac{\partial \mathbf{G}_i^n}{\partial x_i} + \mathbf{B}^n - s_1 \frac{\partial \Delta \mathbf{F}_i^{n+1}}{\partial x_i} - s_3 \frac{\partial \Delta \mathbf{G}_i^{n+1}}{\partial x_i} + s_5 \Delta \mathbf{B}^{n+1} \Bigg] \\ & - \frac{\Delta t^2}{2} \Bigg\{ \Bigg[\frac{\partial}{\partial x_i}(\mathbf{a}_i + \mathbf{b}_i) \left(\frac{\partial \mathbf{F}_j^n}{\partial x_j} + \frac{\partial \mathbf{G}_j^n}{\partial x_j} - \mathbf{B}^n \right) - \mathbf{d} \left(\frac{\partial \mathbf{F}_i^n}{\partial x_i} + \frac{\partial \mathbf{G}_i^n}{\partial x_i} - \mathbf{B}^n \right) \Bigg] \\ & + s_2 \Bigg[\frac{\partial}{\partial x_i}(\mathbf{a}_i + \mathbf{b}_i) \left(\frac{\partial \Delta \mathbf{F}_j^{n+1}}{\partial x_j} \right) - \mathbf{d} \frac{\partial \Delta \mathbf{F}_i^{n+1}}{\partial x_i} \Bigg] + \Bigg[\frac{\partial}{\partial x_i}(\mathbf{a}_i + \mathbf{b}_i) \\ & \times \left(s_4 \frac{\partial \Delta \mathbf{G}_j^{n+1}}{\partial x_j} . - s_6 \Delta \mathbf{B}^{n+1} \right) - \mathbf{d} \left(s_4 \frac{\partial \Delta \mathbf{G}_i^{n+1}}{\partial x_i} . - s_6 \Delta \mathbf{B}^{n+1} \right) \Bigg] \Bigg\} + \mathrm{O}(\Delta \mathrm{t}^3) \end{aligned} \tag{13.6.2a}$$

with the convection, diffusion, and diffusion gradient Jacobians (a_i, b_i, c_{ik}) being defined in (6.3.9) for 2-D and Appendix A for 3-D. The source term Jacobian is given by

$$\mathbf{d} = \frac{\partial \mathbf{B}}{\partial \mathbf{U}}$$

Now, rearranging and expressing the remaining terms associated with the variation parameters in terms of the Jacobians, we have

$$\Delta\mathbf{U}^{n+1} + \Delta t\left[s_1\left(\frac{\partial \mathbf{a}_i \Delta\mathbf{U}^{n+1}}{\partial x_i}\right) + s_3\left(\frac{\partial \mathbf{b}_i \Delta\mathbf{U}^{n+1}}{\partial x_i} + \frac{\partial^2 \mathbf{c}_{ij} \Delta\mathbf{U}^{n+1}}{\partial x_i \partial x_j}\right) - s_5\,\mathbf{d}\Delta U^{n+1}\right]$$
$$- \frac{\Delta t^2}{2}\left\{s_2\left[\frac{\partial^2(\mathbf{a}_i\mathbf{a}_j + \mathbf{b}_i\mathbf{a}_j)\Delta\mathbf{U}^{n+1}}{\partial x_i \partial x_j} - \mathbf{d}\frac{\partial \mathbf{a}_i \Delta\mathbf{U}^{n+1}}{\partial x_i}\right] + s_4\left[\left(\frac{\partial^2(\mathbf{a}_i\mathbf{b}_j + \mathbf{b}_i\mathbf{b}_j)\Delta\mathbf{U}^{n+1}}{\partial x_i \partial x_j}\right)\right.\right.$$
$$\left.\left. - \mathbf{d}\left(\frac{\partial \mathbf{b}_i \Delta\mathbf{U}^{n+1}}{\partial x_i} + \frac{\partial^2 \mathbf{c}_{ij} \Delta\mathbf{U}^{n+1}}{\partial x_i \partial x_j}\right)\right] - s_6\left[\mathbf{d}\frac{\partial(\mathbf{a}_i + \mathbf{b}_i)\Delta\mathbf{U}^{n+1}}{\partial x_i} - \mathbf{d}^2\,\Delta\cup^{n+1}\right]\right\}$$
$$+ \Delta t\left(\frac{\partial \mathbf{F}_i^n}{\partial x_i} + \frac{\partial \mathbf{G}_i^n}{\partial x_i} - \mathbf{B}^n\right) - \frac{\Delta t^2}{2}\left[\frac{\partial}{\partial x_i}(\mathbf{a}_i + \mathbf{b}_i)\left(\frac{\partial \mathbf{F}_j^n}{\partial x_j} + \frac{\partial \mathbf{G}_j^n}{\partial x_j} - \mathbf{B}^n\right)\right.$$
$$\left. - \mathbf{d}\left(\frac{\partial \mathbf{F}_i^n}{\partial x_i} + \frac{\partial \mathbf{G}_i^n}{\partial x_i} - \mathbf{B}^n\right)\right] + \mathrm{O}(\Delta t^3) = 0 \tag{13.6.2b}$$

with

$$\Delta\mathbf{B}^{n+1} = \frac{\partial \mathbf{B}}{\partial \mathbf{U}}\Delta\mathbf{U}^{n+1} = \mathbf{d}\Delta\mathbf{U}^{n+1} \tag{13.6.3}$$

Here, the product of the diffusion gradient Jacobian with third order spatial derivatives is neglected and all Jacobians a_i, b_i, c_{ij}, and d are assumed to remain constant spatially within each time step and to be updated at subsequent time steps. The FDV parameters s_1, s_2, s_3, s_4 are defined in Section 6.5.1 and Figures 6.5.1 through 6.5.3. Additional parameters for source terms s_5, s_6 are defined in a similar manner:

$$\begin{aligned} s_a\Delta\mathbf{B} &\Rightarrow s_5\Delta\mathbf{B} \\ s_b\Delta\mathbf{B} &\Rightarrow s_6\Delta\mathbf{B} \end{aligned} \tag{13.6.4}$$

where the source term FDV parameters s_5 (first order source term FDV parameter) and s_6 second order source term FDV parameter) are evaluated as

$$s_5 = \begin{cases} \min(r,\ 1) & r > \alpha, \quad \alpha \cong 0.01 \\ 0 & r < \alpha, \quad Da_{\min} \neq 0 \\ 1 & Da_{\min} = 0 \end{cases} \tag{13.6.5a}$$

$$s_6 = \frac{1}{2}\left(1 + s_5^{\eta}\right), \quad 0.05 < \eta < 0.2 \tag{13.6.5b}$$

with

$$r = \sqrt{Da_{\max}^2 - Da_{\min}^2}\Big/ Da_{\min} \tag{13.6.5c}$$

where the Damköhler number Da can be defined in five different ways as shown in Table 22.2.1.

For simplicity, we may rearrange (13.6.2b) in a compact form,

$$\mathbf{R} = \mathbf{A}\Delta\mathbf{U}^{n+1} + \frac{\partial}{\partial x_i}\left(\mathbf{E}_i\,\Delta\mathbf{U}^{n+1}\right) + \frac{\partial^2}{\partial x_i \partial x_j}\left(\mathbf{E}_{ij}\,\Delta\mathbf{U}^{n+1}\right) + \mathbf{Q}^n + \mathrm{O}(\Delta t^3), \tag{13.6.6}$$

or, lagging E_i and E_{ij} one time step behind,

$$\left(\mathbf{A}+\mathbf{E}_i^n\frac{\partial}{\partial x_i}+\mathbf{E}_{ij}^n\frac{\partial^2}{\partial x_i\partial x_j}\right)\Delta\mathbf{U}^{n+1}=-\mathbf{Q}^n \tag{13.6.7}$$

with

$$\mathbf{A}=\mathbf{I}-\Delta t\,s_5\,\mathbf{d}-\frac{\Delta t^2}{2}s_6\,\mathbf{d}^2 \tag{13.6.8a}$$

$$\mathbf{E}_i^n=\left\{\Delta t(s_1\mathbf{a}_i+s_3\mathbf{b}_i)+\frac{\Delta t^2}{2}[s_6\,\mathbf{d}(\mathbf{a}_i+\mathbf{b}_i)+s_2\,\mathbf{d}\mathbf{a}_i+s_4\mathbf{d}\mathbf{b}_i]\right\}^n \tag{13.6.8b}$$

$$\mathbf{E}_{ij}^n=\left\{\Delta t\,s_3\mathbf{c}_{ij}-\frac{\Delta t^2}{2}[s_2(\mathbf{a}_i\mathbf{a}_j+\mathbf{b}_i\mathbf{a}_j)+s_4(\mathbf{a}_i\mathbf{b}_j+\mathbf{b}_i\mathbf{b}_j-\mathbf{d}\mathbf{c}_{ij})]\right\}^n \tag{13.6.8c}$$

$$\begin{aligned}\mathbf{Q}^n=&\frac{\partial}{\partial x_i}\left[\left(\Delta t+\frac{\Delta t^2}{2}\mathbf{d}\right)(\mathbf{F}_i^n+\mathbf{G}_i^n)+\frac{\Delta t^2}{2}(\mathbf{a}_i+\mathbf{b}_i)\mathbf{B}^n\right]\\&-\frac{\partial^2}{\partial x_i\partial x_j}\left[\frac{\Delta t^2}{2}(\mathbf{a}_i+\mathbf{b}_i)(\mathbf{F}_j^n+\mathbf{G}_j^n)\right]-\left(\Delta t+\frac{\Delta t^2}{2}\mathbf{d}\right)\mathbf{B}^n\end{aligned} \tag{13.6.8d}$$

An alternative scheme is to allow the source term in the left-hand side of (13.6.7) to lag from $n+1$ to n so that (13.6.7) may be written as

$$\left(\mathbf{I}+\mathbf{E}_i^n\frac{\partial}{\partial x_i}+\mathbf{E}_{ij}^n\frac{\partial^2}{\partial x_i\partial x_j}\right)\Delta\mathbf{U}^{n+1}=-\mathbf{Q}^n \tag{13.6.9}$$

$$\begin{aligned}\mathbf{Q}^n=&\frac{\partial}{\partial x_i}\left[\left(\Delta t+\frac{\Delta t^2}{2}\mathbf{d}\right)(\mathbf{F}_i^n+\mathbf{G}_i^n)+\frac{\Delta t^2}{2}(\mathbf{a}_i+\mathbf{b}_i)\mathbf{B}^n\right]-\frac{\partial^2}{\partial x_i\partial x_j}\\&\times\left[\frac{\Delta t^2}{2}(\mathbf{a}_i+\mathbf{b}_i)(\mathbf{F}_j^n+\mathbf{G}_j^n)\right]-\left(\Delta t\,s_5+\frac{\Delta t^2}{2}s_6\mathbf{d}\right)\mathbf{d}\Delta\mathbf{U}^n-\left(\Delta t+\frac{\Delta t^2}{2}\mathbf{d}\right)\mathbf{B}^n\end{aligned} \tag{13.6.10}$$

13.6.2 INTERPRETATION OF FDV PARAMETERS ASSOCIATED WITH JACOBIANS

The flowfield-dependent FDV parameters as defined earlier are capable of allowing various numerical schemes to be automatically generated as summarized in Section 6.5.4. For the purpose of completeness and emphasis, they are repeated here along with additional features associated with FEM and the source terms.

The first order FDV parameters s_1 and s_3 control all high-gradient phenomena such as shock waves and turbulence. These parameters as calculated from the changes of local Mach numbers, and Reynolds (or Peclet) numbers between adjacent nodes are indicative of the actual local element flowfields. The contours of these parameters closely resemble the flowfields themselves, with both s_1 and s_3 being large (close to unity) in regions of high gradients, but small (close to zero) in regions where the gradients are small (see Figures 6.5.1 through 6.5.3).

The second order FDV parameters s_2 and s_4 are also flowfield dependent, exponentially proportional to the first order FDV parameters. However, their primary role is to provide adequate computational stability (artificial viscosity) as they were originally

introduced into the second order time derivative term of the Taylor series expansion of the conservation flow variables $\mathbf{U}^{n+1}$.

The s_1 terms represent convection. This implies that if $s_1 \cong 0$, then the effect of convection is small. The computational scheme is automatically altered to take this effect into account, with the governing equations being predominantly parabolic-elliptic. The s_3 terms are associated with diffusion. Thus, with $s_3 \cong 0$, the effect of viscosity or diffusion is small and the computational scheme is automatically switched to that of Euler equations where the governing equations are predominantly hyperbolic. If the first order variation parameters s_1 and s_3 are nonzero, this indicates a typical situation for the mixed hyperbolic, parabolic, and elliptic nature of the Navier-Stokes system of equations, with convection and diffusion being equally important. This is the case for incompressible flows at low speeds.

The unique property of the FDV scheme is its capability to control pressure oscillations adequately without resorting to the separate hyperbolic-elliptic pressure equation for pressure corrections. The capability of the FDV scheme to handle incompressible flows is achieved by a delicate balance between s_1 and s_3 as determined by the local Mach numbers and Reynolds (or Peclet) numbers. If the flow is completely incompressible ($M = 0$), the criteria given by (13.6.9) leads to $s_1 = 1$, whereas the FDV parameter s_3 is to be determined according to the criteria given in (13.6.11). Make a note of the presence of the convection-diffusion interaction terms given by the product of $b_i a_j$ in the s_2 terms and $a_i b_j$ in the s_4 terms. These terms allow interactions between convection and diffusion in the viscous incompressible and/or viscous compressible flows.

If temperature gradients rather than velocity gradients dominate the flowfield, then s_3 is governed by the Peclet number rather than by the Reynolds number. Such cases arise in high-speed, high-temperature compressible flows close to the wall.

The transition to turbulence is a natural flow process as the Reynolds number increases, causing the gradients of any or all flow variables to increase. This phenomenon is a physical instability and is detected by the increase of s_3 if the flow is incompressible, but by both s_3 and s_1 if the flow is compressible. Such physical instability is likely to trigger the numerical instability, but will be countered by the second order variation parameters s_2 and/or s_4 to ensure numerical stability automatically. In this process, these flowfield dependent variation parameters are capable of capturing relaminarization, compressibility effect or dilatational turbulent energy dissipation, and turbulent unsteady fluctuations. These physical phenomena are originated from transitions and interactions between inviscid and viscous flows. They are characterized by the product of s_3 and the fluctuation stress tensor ($s_3 \tau_{ij}$) in which the stresses consist of mean and fluctuation parts. As a consequence, $\Delta \mathbf{U}^{n+1}$ in (13.6.3) or (13.6.5) may not uniformly vanish, indicating that some regions of the domain (such as in the boundary layers) remain unsteady if the flow is turbulent. However, if turbulent microscales (Kolmogorov microscale) are to be resolved, then we must allow mesh refinements normally required for the direct numerical simulation (DNS).

A unique feature in finite element applications of the FDV theory is the FDV parameters, which can be used as error indicators for adaptive meshing. The source terms such as those contributing to the finite rate chemistry were not included in Section 6.5. These topics are elaborated next.

FDV Parameters Used as Error Indicators for Adaptive Mesh. An important contribution of the first and second order FDV parameters is the fact that they can be used as error indicators for adaptive mesh generations (see Figure 19.2.5, Section 19.2.1). That is, the larger the FDV parameters, the higher the gradients of any flow variables. Whichever governs (largest first or second order variation parameters) will indicate the need for mesh refinements. In this case, all variables (density, velocity, pressure, temperature, species mass fraction) participate in resolving the adaptive mesh, contrary to the conventional definitions of the error indicators.

Finite Rate Chemistry. In the case of reacting flows, the source term **B** contains the reaction rates which are functions of the flowfield variables. With widely disparate time and length scales involved in the fast and slow chemical reaction rates of various chemical species as characterized by Damköhler numbers, the first order source term variation parameter s_5 is instrumental in dealing with the stiffness of the resulting equations to obtain convergence to accurate solutions. On the other hand, the second order source term FDV parameter s_6 contributes to the stability of solutions. It is seen that the criteria given by (13.6.5) will adjust the reaction rate terms in accordance with the ratio of the diffusion time to the reaction time in finite rate chemistry so as to assure the accurate solutions in dealing with stiffness and computational stability.

Influence of FDV Parameters on Jacobians. Physically, the FDV parameters will influence the magnitudes of Jacobians. The diffusion variation parameters s_3 and s_4 as calculated from Reynolds number and Peclet number can be applied to the Jacobians (a_i, b_i, c_{ij}), corresponding to the momentum equations and energy equation, respectively. Furthermore, two different definitions of Peclet number ($\mathrm{Pe_I}$, $\mathrm{Pe_{II}}$) (see Table 22.2.1) would require the s_3 and s_4 as calculated from the energy and species equations to be applied to the corresponding terms of the Jacobians. Similar applications for the source term variation parameters s_5 and s_6 should be followed for the source term Jacobian d, based on the various definitions of Damköhler number (Da_I, Da_{II}, Da_{III}, Da_{IV}, Da_V) as shown in Table 22.2.1. In this way, high temperature gradients arising from the momentum and energy equations and the finite rate chemistry governed by the energy and species equations can be resolved accordingly.

13.6.3 NUMERICAL DIFFUSION

Note that the numerical diffusion is implicitly embedded in the FDV equations. This can be demonstrated by writing (13.6.2a) separately for the equations of momentum, continuity, and energy. Combining the momentum and continuity equations and reconstructing the original differential equations, we identify the numerical diffusion terms which are produced for all governing equations as a consequence of FDV formulations. We summarize the reconstructed equations of momentum, continuity, and energy without the source terms from (6.5.25), (6.5.28), (6.5.31). It is interesting to note that if we neglect all incremental (fluctuation) terms, we arrive at the results identical or analogous to many of the recent developments in FEM for the treatment of convection dominated flows, including the generalized Petrov-Galerkin (GPG) methods,

characteristic Galerkin methods (CGM), etc., presented in the previous chapters. To demonstrate this analogy, let us neglect all incremental and higher order terms, but retain only the second order derivative terms, with $s_1 = 1/2$, so that we may arrive at the form more easily recognizable. Here, all components of convection and diffusion Jacobians can be shown to be the velocity components, $a_i^{(m)} = a_i^{(c)} = a_i^{(e)} = \mathrm{v}_i$. These arrangements lead to

Momentum

$$\frac{\partial}{\partial t}(\rho \mathrm{v}_j) + (\rho \mathrm{v}_i \mathrm{v}_j)_{,i} + p_{,j} - \tau_{ij,i} = S_j(m) \tag{13.6.11}$$

with

$$S_j(m) = \frac{\Delta t}{2}[\mathrm{v}_k (\rho \mathrm{v}_i \mathrm{v}_j + p\delta_{ij} - \tau_{ij})_{,i}]_{,k} \tag{13.6.12}$$

Continuity

$$\frac{\partial \rho}{\partial t} + (\rho \mathrm{v}_i)_{,i} = S(c) \tag{13.6.13}$$

with

$$S(c) = \frac{\Delta t}{2}[(\rho \mathrm{v}_i \mathrm{v}_j)_{,ij} + p_{,jj} - \tau_{ij,ij} + (\mathrm{v}_i(\rho \mathrm{v}_j)_{,j})_{,i}] \tag{13.6.14}$$

Energy

$$\frac{\partial}{\partial t}(\rho E) + [(\rho E + p)\mathrm{v}_i - kT_{,i} - \tau_{ij}\mathrm{v}_j]_{,i} = S(e) \tag{13.6.15}$$

with

$$S(e) = \frac{\Delta t}{2}\{\mathrm{v}_k[((\rho E + p)\mathrm{v}_i)_{,i} - kT_{,ii} - (\tau_{ij}\mathrm{v}_j)_{,i}]\}_{,k} \tag{13.6.16}$$

Examining the right-hand side terms for all equations, they are identified as numerical diffusions which arise from GPG or CGM formulations. It is seen that second derivatives of pressure arise on the right-hand side explicitly. Direct comparisons can be made with reference to CGM through (13.4.9) through (13.4.14).

13.6.4 TRANSITIONS AND INTERACTIONS BETWEEN COMPRESSIBLE AND INCOMPRESSIBLE FLOWS AND BETWEEN LAMINAR AND TURBULENT FLOWS

In order to understand how the FDV scheme handles computations involving both compressible and incompressible flows, fundamental definitions of pressure as involved in compressible and incompressible flows must be recognized, as pointed out in Section 6.5.6. In view of (6.5.33) through (6.5.36), we note that, if p_o as given by (6.5.36) remains a constant, equivalent to a stagnation (total) pressure, then the compressible flow as assumed in the conservation form of the Navier-Stokes system of equations has now been turned into an incompressible flow, which is expected to occur when the flow velocity is sufficiently reduced (approximately $0.1 \leq M < 0.3$ for air). Thus, (6.6.36) serves as an equivalent equation of state for an incompressible flow. This can be identified nodal point by nodal point or element by element for the entire domain.

When inviscid flow becomes viscous, we may expect that the flow may become laminar or turbulent through inviscid/viscous interactions across the boundary layer. Below the laminar boundary layer, if viscous actions are significant, then the fluid particles are unstable, causing the changes of Mach number and Reynolds number between adjacent nodal points (assuming they are closely spaced) to be irregular, the phenomenon known as transition instability prior to the state of full turbulence. Fluctuations due to turbulence are characterized by the presence of the terms such as in (6.5.37). Physically, this quantity represents the fluctuations of total stresses (physical viscous stresses plus Reynolds stresses) controlled by the Reynolds number changes between the local adjacent nodal points. Thus, the FDV solution contains the sum of the mean flow variables and the fluctuation parts of the variables. Once the solution of the Navier-Stokes system of equations is carried out and all flow variables are determined, then we compute the fluctuation part, f' of any variable f, as given in (6.5.38). Unsteady turbulence statistics (turbulent kinetic energy, Reynolds stresses, and various energy spectra) can be calculated once the fluctuation quantities of all variables are determined. Although the solutions of the Navier-Stokes system of equations using FDV are assumed to contain the fluctuation parts as well as the mean quantities, it will be unlikely that such information is reliable when the Reynolds number is very high and if mesh refinements are not adequate to resolve Kolmogorov microscales. In this case, it is necessary to invoke the level of mesh refinements as required for DNS.

Unsteadiness in turbulent fluctuations may prevail in the vicinity of the wall, although a steady-state may have been reached far away from the wall. This situation can easily be verified by noting that $\Delta\mathbf{U}^{n+1}$ will vanish only in the region far away from the wall, but remain fluctuating in the vicinity of the wall, as dictated by the changes of Mach number in the variation parameter s_3 between the nodal points and fluctuations of the stresses due to both physical and turbulent viscosities in $\Delta\tau_{ij}$ characterized by (6.5.37).

13.6.5 FINITE ELEMENT FORMULATION OF FDV EQUATIONS

We recall that all the provisions and numerical aspects for the physical phenomena such as discontinuities and fluctuations of flow variables have already been incorporated in the FDV equations. The standard Galerkin integral formulations of the FDV equations are all that will be necessary. Thus, we begin by expressing the conservation and flux variables and source terms as a linear combination of trial functions Φ_α with the nodal values of these variables in the form,

$$\mathbf{U}(\mathbf{x}, t) = \Phi_\alpha(\mathbf{x})\mathbf{U}_\alpha(t), \qquad \mathbf{F}_i(\mathbf{x}, t) = \Phi_\alpha(\mathbf{x})\mathbf{F}_{\alpha i}(t)$$
$$\mathbf{G}_i(\mathbf{x}, t) = \Phi_\alpha(\mathbf{x})\mathbf{G}_{\alpha i}(t), \qquad \mathbf{B}(\mathbf{x}, t) = \Phi_\alpha(\mathbf{x})\mathbf{B}_\alpha(t)$$

Applying the standard Galerkin approximations to (13.6.7), we obtain

$$\int_\Omega \Phi_\alpha \mathbf{R}(\mathbf{U}, \mathbf{F}_i, \mathbf{G}_i, \mathbf{B})\, d\Omega = 0 \tag{13.6.17}$$

or

$$(A_{\alpha\beta}\eta_{rs} + B_{\alpha\beta rs})\,\Delta U^{n+1}_{\beta s} = H^n_{\alpha r} + N^n_{\alpha r} \tag{13.6.18}$$

where

$$A_{\alpha\beta} = \int_\Omega \Phi_\alpha \Phi_\beta \, d\Omega, \quad \eta_{rs} = \delta_{rs} + \Delta t \, s_5 \, d_{rs} + \frac{\Delta t^2}{2} s_6 \, d_{rm} \, d_{ms} \tag{13.6.19}$$

$$\begin{aligned} B_{\alpha\beta rs} = \int_\Omega \Bigg[& - \left\{ \Delta t (s_1 a_{irs} + s_3 \, b_{irs}) + \frac{\Delta t^2}{2} [s_2 d_{rt} a_{its} + s_6 d_{rt} \, (a_{its} + b_{its}) + s_4 d_{rt} b_{its}] \right\} \\ & \times \Phi_{\alpha,i} \Phi_\beta - \left\{ \Delta t \, s_3 c_{ijrs} - \frac{\Delta t^2}{2} [s_2 (a_{irt} a_{jts} + b_{irt} a_{jts}) + s_4 (a_{irt} b_{jts} + b_{irt} b_{jts} \right. \\ & \left. - d_{rt} c_{ijts})] \right\} \Phi_{\alpha,i} \Phi_{\beta,j} \Bigg] d\,\Omega + \int_\Gamma \Bigg[\left\{ \Delta t (s_1 a_{irs} + s_3 \, b_{irs}) + \frac{\Delta t^2}{2} [s_2 d_{rt} a_{its} \right. \\ & \left. + s_6 d_{rt} \, (a_{its} + b_{its}) + s_4 d_{rt} b_{its}] \right\} \overset{*}{\Phi}_\alpha \overset{*}{\Phi}_\beta + \left\{ \Delta t \, s_3 c_{ijrs} - \frac{\Delta t^2}{2} [s_2 (a_{irt} a_{jts} \right. \\ & \left. + b_{irt} a_{jts}) + s_4 (a_{irt} b_{jts} + b_{irt} b_{jts} - d_{rt} c_{ijts})] \right\} \overset{*}{\Phi}_\alpha \overset{*}{\Phi}_{\beta,j} \Bigg] n_i \, d\,\Gamma \end{aligned} \tag{13.6.20}$$

$$\begin{aligned} H^n_{\alpha r} = \int_\Omega \Bigg\{ & \left[\Delta t \left(F^n_{\beta ir} + G^n_{\beta ir} \right) + \frac{\Delta t^2}{2} d_{rs} \left(F^n_{\beta is} + G^n_{\beta is} \right) + \frac{\Delta t^2}{2} (a_{irs} + b_{irs}) B^n_{\beta s} \right] \Phi_{\alpha,i} \Phi_\beta \\ & - \frac{\Delta t^2}{2} (a_{irs} + b_{irs}) \left(F^n_{\beta js} + G^n_{\beta js} \right) \Phi_{\alpha,i} \Phi_{\beta,j} + \left[\Delta t \, B^n_{\beta r} + \frac{\Delta t^2}{2} d_{rs} B^n_{\beta s} \right] \Phi_\alpha \Phi_\beta \Bigg\} d\Omega \end{aligned} \tag{13.6.21}$$

$$\begin{aligned} N^n_{\alpha r} = \int_\Gamma \Bigg\{ & \left[- \Delta t \left(F^n_{\beta ir} + G^n_{\beta ir} \right) - \frac{\Delta t^2}{2} d_{rs} \left(F^n_{\beta is} + G^n_{\beta is} \right) - \frac{\Delta t^2}{2} (a_{irs} + b_{irs}) B^n_{\beta s} \right] \overset{*}{\Phi}_\alpha \overset{*}{\Phi}_\beta \\ & + \frac{\Delta t^2}{2} (a_{irs} + b_{irs}) \left(F^n_{\beta js} + G^n_{\beta js} \right) \overset{*}{\Phi}_\alpha \overset{*}{\Phi}_{\beta,j} \Bigg\} n_i \, d\Gamma \end{aligned} \tag{13.6.22}$$

Here all Jacobians must be updated at each iteration step, $\overset{*}{\Phi}_\alpha$ represents the Neumann boundary trial and test functions, with α, β denoting the global node number and r, s providing the number of conservation variables at each node. For three dimensions, i, $j = 1, 2, 3$ associated with the Jacobians imply directional identification of each Jacobian matrix $(a_1, a_2, a_3, b_1, b_2, b_3, c_{11}, c_{12}, c_{13}, c_{21}, c_{22}, c_{23}, c_{31}, c_{32}, c_{33})$ with $r, s = 1, 2, 3, 4, 5$ denoting entries of each of the 5×5 Jacobian matrices. These indices can be reduced similarly for 2-D.

Evaluation of integrals in (13.6.19)–(13.6.22) must begin with local elements of the form

$$\left(A^{(e)}_{NM} \delta_{rs} + B^{(e)}_{NMrs} \right) \Delta U^{(e)}_{Ms} = H^{n(e)}_{Nr} + N^{n(e)}_{Nr}$$

We shall describe the procedure for two-dimensional isoparametric elements using Gaussian quadrature integrations with an EBE process for assembly into a global form as shown in Section 10.3.2. The local FDV finite element equation given above represents a system of 16 equations with N, $M = 1, 2, 3, 4$ and $r, s = 1, 2, 3, 4$. These matrix equations are constructed by summing terms with repeated indices. A simple computer

algorithm can be developed to achieve this process. For example, $A^{(e)}_{NM}\delta_{rs}\Delta U^{(e)}_{Ms}$ takes the form

$$\begin{bmatrix}
A_{11} & & & A_{12} & & & A_{13} & & & A_{14} & & & \\
 & A_{11} & & & A_{12} & & & A_{13} & & & A_{14} & & \\
 & & A_{11} & & & A_{12} & & & A_{13} & & & A_{14} & \\
 & & & A_{11} & & & A_{12} & & & A_{13} & & & A_{14} \\
A_{21} & & & A_{22} & & & A_{23} & & & A_{24} & & & \\
 & A_{21} & & & A_{22} & & & A_{23} & & & A_{24} & & \\
 & & A_{21} & & & A_{22} & & & A_{23} & & & A_{24} & \\
 & & & A_{21} & & & A_{22} & & & A_{23} & & & A_{24} \\
A_{31} & & & A_{32} & & & A_{33} & & & A_{34} & & & \\
 & A_{31} & & & A_{32} & & & A_{33} & & & A_{34} & & \\
 & & A_{31} & & & A_{32} & & & A_{33} & & & A_{34} & \\
 & & & A_{31} & & & A_{32} & & & A_{33} & & & A_{34} \\
A_{41} & & & A_{42} & & & A_{43} & & & A_{44} & & & \\
 & A_{41} & & & A_{42} & & & A_{43} & & & A_{44} & & \\
 & & A_{41} & & & A_{42} & & & A_{43} & & & A_{44} & \\
 & & & A_{41} & & & A_{42} & & & A_{43} & & & A_{44}
\end{bmatrix}
\begin{bmatrix}
\Delta U_{11} \\ \Delta U_{12} \\ \Delta U_{13} \\ \Delta U_{14} \\ \Delta U_{21} \\ \Delta U_{22} \\ \Delta U_{23} \\ \Delta U_{24} \\ \Delta U_{31} \\ \Delta U_{32} \\ \Delta U_{33} \\ \Delta U_{34} \\ \Delta U_{41} \\ \Delta U_{42} \\ \Delta U_{43} \\ \Delta U_{44}
\end{bmatrix}$$

Similarly, $B^{(e)}_{NMrs}\Delta U^{(e)}_{Ms}$ is of the form

$$\begin{bmatrix}
B_{1111} & B_{1112} & B_{1113} & B_{1114} & B_{1211} & B_{1212} & B_{1213} & B_{1214} & B_{1311} & B_{1312} & B_{1313} & B_{1314} & B_{1411} & B_{1412} & B_{1413} & B_{1414} \\
B_{1121} & B_{1122} & B_{1123} & B_{1124} & B_{1221} & B_{1222} & B_{1223} & B_{1224} & B_{1321} & B_{1322} & B_{1323} & B_{1324} & B_{1421} & B_{1422} & B_{1423} & B_{1424} \\
B_{1131} & B_{1132} & B_{1133} & B_{1134} & B_{1231} & B_{1232} & B_{1233} & B_{1234} & B_{1331} & B_{1332} & B_{1333} & B_{1334} & B_{1431} & B_{1432} & B_{1433} & B_{1434} \\
B_{1141} & B_{1142} & B_{1143} & B_{1144} & B_{1241} & B_{1242} & B_{1243} & B_{1244} & B_{1341} & B_{1342} & B_{1343} & B_{1344} & B_{1441} & B_{1442} & B_{1443} & B_{1444} \\
B_{2111} & B_{2112} & B_{2113} & B_{2114} & B_{2211} & B_{2212} & B_{2213} & B_{2214} & B_{2311} & B_{2312} & B_{2313} & B_{2314} & B_{2411} & B_{2412} & B_{2413} & B_{2414} \\
B_{2121} & B_{2122} & B_{2123} & B_{2124} & B_{2221} & B_{2222} & B_{2223} & B_{2224} & B_{2321} & B_{2322} & B_{2323} & B_{2324} & B_{2421} & B_{2422} & B_{2423} & B_{2424} \\
B_{2131} & B_{2132} & B_{2133} & B_{2134} & B_{2231} & B_{2232} & B_{2233} & B_{2234} & B_{2331} & B_{2332} & B_{2333} & B_{2334} & B_{2431} & B_{2432} & B_{2433} & B_{2434} \\
B_{2141} & B_{2142} & B_{2143} & B_{2144} & B_{2241} & B_{2242} & B_{2243} & B_{2244} & B_{2341} & B_{2342} & B_{2343} & B_{2344} & B_{2441} & B_{2442} & B_{2443} & B_{2444} \\
B_{3111} & B_{3112} & B_{3113} & B_{3114} & B_{3211} & B_{3212} & B_{3213} & B_{3214} & B_{3311} & B_{3312} & B_{3313} & B_{3314} & B_{3411} & B_{3412} & B_{3413} & B_{3414} \\
B_{3121} & B_{3122} & B_{3123} & B_{3124} & B_{3221} & B_{3222} & B_{3223} & B_{3224} & B_{3321} & B_{3322} & B_{3323} & B_{3324} & B_{3421} & B_{3422} & B_{3423} & B_{3424} \\
B_{3131} & B_{3132} & B_{3133} & B_{3134} & B_{3231} & B_{3232} & B_{3233} & B_{3234} & B_{3331} & B_{3332} & B_{3333} & B_{3334} & B_{3431} & B_{3432} & B_{3433} & B_{3434} \\
B_{3141} & B_{3142} & B_{3143} & B_{3144} & B_{3241} & B_{3242} & B_{3243} & B_{3244} & B_{3341} & B_{3342} & B_{3343} & B_{3344} & B_{3441} & B_{3442} & B_{3443} & B_{3444} \\
B_{4111} & B_{4112} & B_{4113} & B_{4114} & B_{4211} & B_{4212} & B_{4213} & B_{4214} & B_{4311} & B_{4312} & B_{4313} & B_{4314} & B_{4411} & B_{4412} & B_{4413} & B_{4414} \\
B_{4121} & B_{4122} & B_{4123} & B_{4124} & B_{4221} & B_{4222} & B_{4223} & B_{4224} & B_{4321} & B_{4322} & B_{4323} & B_{4324} & B_{4421} & B_{4422} & B_{4423} & B_{4424} \\
B_{4131} & B_{4132} & B_{4133} & B_{4134} & B_{4231} & B_{4232} & B_{4233} & B_{4234} & B_{4331} & B_{4332} & B_{4333} & B_{4334} & B_{4431} & B_{4432} & B_{4433} & B_{4434} \\
B_{4141} & B_{4142} & B_{4143} & B_{4144} & B_{4241} & B_{4242} & B_{4243} & B_{4244} & B_{4341} & B_{4342} & B_{4343} & B_{4344} & B_{4441} & B_{4442} & B_{4443} & B_{4444}
\end{bmatrix}
\begin{bmatrix}
\Delta U_{11} \\ \Delta U_{12} \\ \Delta U_{13} \\ \Delta U_{14} \\ \Delta U_{21} \\ \Delta U_{22} \\ \Delta U_{23} \\ \Delta U_{24} \\ \Delta U_{31} \\ \Delta U_{32} \\ \Delta U_{33} \\ \Delta U_{34} \\ \Delta U_{41} \\ \Delta U_{42} \\ \Delta U_{43} \\ \Delta U_{44}
\end{bmatrix}$$

For example, let us examine one of the terms in B_{1214},

$$B_{1214} = \frac{\Delta t^2}{2}\int_\Omega s_2 a_{i1t} a_{jt4} \Phi_{1,i} \Phi_{2,j} d\Omega + \cdots \quad \text{with } i, j = 1, 2, \quad t = 1, 2, 3, 4$$

All integrals are to be integrated using Gaussian quadrature.

The domain integrals on the right-hand side are evaluated similarly. However, they will result in a column vector compatible with left-hand side.

The evaluation of boundary integrals that appear in both left-hand side and right-hand side are discussed in the next section.

13.6.6 BOUNDARY CONDITIONS

Treatment of boundary conditions in finite element methods is simple and straightforward as discussed in Section 10.1.2. Particularly, in FDV formulations where all regimes of velocity are to be accommodated in multidimensions, implementations of boundary conditions are self-explanatory. Neumann boundary conditions in FDV occur in both left-hand side and right-hand side. The left-hand side Neumann boundary integrals are evaluated and summed into the corresponding domain integrals as first discussed in Section 10.2.4, whereas the right-hand side Neumann boundary conditions appear as a column vector as shown in Section 10.1.3.

The Neumann boundary conditions

To illustrate, let us consider one of the boundary integrals multiplied by the conservation variable vector on the left-hand side.

(1) $N = 1, r = 1, M = 1, 2, s = 1, 2, 3, 4,\ i, j = 1, 2$

$$\int_\Gamma a_{irs} \overset{*}{\Phi}_N \overset{*}{\Phi}_M n_i d\Gamma \Delta U_{Ms} = \int_\Gamma \{(a_{111}n_1 + a_{211}n_2)\Delta U_{11} + (a_{112}n_1 + a_{212}n_2)\Delta U_{12}$$
$$+(a_{113}n_1 + a_{213}n_2)\Delta U_{13} + (a_{114}n_1 + a_{214}n_2)\Delta U_{14}\} \overset{*}{\Phi}_1 \overset{*}{\Phi}_1 d\Gamma$$
$$+ \int_\Gamma \{(a_{111}n_1 + a_{211}n_2)\Delta U_{21} + (a_{112}n_1 + a_{212}n_2)\Delta U_{22}$$
$$+(a_{113}n_1 + a_{214}n_2)\Delta U_{23} + (a_{114}n_1 + a_{214}n_2)\Delta U_{24}\} \overset{*}{\Phi}_1 \overset{*}{\Phi}_2 d\Gamma$$

(2) $N = 1, r = 2, M = 1, 2, s = 1, 2, 3, 4,\ i, j = 1, 2$

(3) $N = 1, r = 3, M = 1, 2, s = 1, 2, 3, 4,\ i, j = 1, 2$

(4) $N = 1, r = 4, M = 1, 2, s = 1, 2, 3, 4,\ i, j = 1, 2$

(5) $N = 2, r = 1, M = 1, 2, s = 1, 2, 3, 4,\ i, j = 1, 2$

(6) $N = 2, r = 2, M = 1, 2, s = 1, 2, 3, 4,\ i, j = 1, 2$

(7) $N = 2, r = 3, M = 1, 2, s = 1, 2, 3, 4,\ i, j = 1, 2$

(8) $N = 2, r = 4, M = 1, 2, s = 1, 2, 3, 4,\ i, j = 1, 2$

Note that the terms with repeated indices will be summed for the free indices $N = 1, 2$ and $r = 1, 2, 3, 4$ for the two-node boundary line elements, resulting in the 8×8 square matrix corresponding to the $8 \times 1 \Delta U_{Ms}$ (see Figures 10.1.2 and 13.6.1). If two nodes, node 1 and node 2, of the boundary line element coincide with node 1 and node 2 of the local element adjoining the boundary line shown in Figure 13.6.1, then the 8×8 boundary line element matrix is algebraically added to the corresponding 16×16 local element matrix. This is the influence of the boundary conditions affecting the domain at the current time step $n + 1$.

The situation is different for the case of the right-hand side boundary integrals at the time step n. They simply result in a column vector as is the case for the regular time-dependent finite element equations. Note also that various Jacobians are

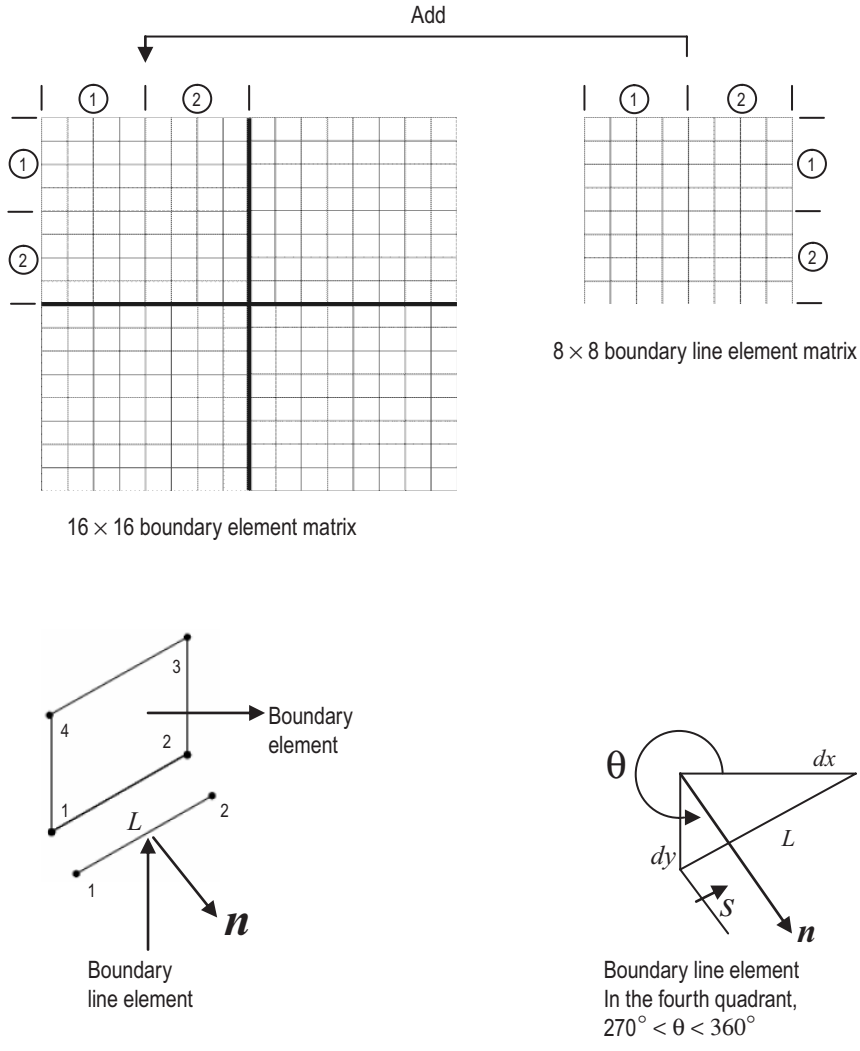

Figure 13.6.1 The 8×8 boundary line element matrix added to the adjoining 16×16 boundary element matrix for the left-hand side boundary integral terms.

multiplied by convection flux variables and diffusion flux variables, indicating that not only the boundary values within the Jacobians but also the flux variable as specified at the boundary nodes are to influence the outcome of the CFD solution.

It should be noted that one of the advantages of the FDV approach is the ability to specify all the values that occur in the Jacobians (a_i, b_i, c_{ij}) and flux variables (F_i, G_i) at the boundary nodes. For example, primitive variables (Dirichlet boundary conditions) and their gradients can be specified at boundary nodes directly through the Jacobians and flux variables.

To illustrate the boundary integrals with derivatives of trial functions, we consider a typical case as in Figure 13.6.1.

$$\int_{\Gamma} a_{irs} F^{n}_{Mjs} \overset{*}{\Phi}_{N} \overset{*}{\Phi}_{M,j} n_i d\Gamma$$

Using Figure 10.1.2b or Figure 13.6.1, let us examine the following integrals:

$$\int_\Gamma \overset{*}{\Phi}_1 \overset{*}{\Phi}_{1,1} n_1 d\Gamma = \int_0^L \overset{*}{\Phi}_1 \frac{\partial \overset{*}{\Phi}_1}{\partial s} \frac{\partial s}{\partial x} \cos\theta ds, \qquad \overset{*}{\Phi}_1 = \left(1 - \frac{s}{L}\right)$$

$$\int_\Gamma \overset{*}{\Phi}_1 \overset{*}{\Phi}_{1,2} n_2 d\Gamma = \int_0^L \overset{*}{\Phi}_1 \frac{\partial \overset{*}{\Phi}_{21}}{\partial s} \frac{\partial s}{\partial y} \sin\theta ds, \qquad \overset{*}{\Phi}_2 = \left(\frac{s}{L}\right)$$

Notice that $\partial s/\partial x = 1/\cos\theta$ and $\partial s/\partial y = 1/\sin\theta$ lead to indeterminate forms when dealing with horizontal or vertical boundary lines ($\theta = 0°, 90°$). The boundary integrals should be set equal to zero when these conditions arise.

The Dirichlet boundary conditions

Implementations of Dirichlet boundary conditions as discussed in Section 10.1.2 cannot be applied. This is because the solution vector is in terms of the incremental conservation flow variables $\Delta U_{\beta s}^{n+1}$. At the boundary nodes with Dirichlet data (constant throughout the entire process), we have $\Delta U^{n+1} = U^{n+1} - U^n = 0$. This must be verified at each time step. As seen already for the case of Neumann boundary conditions, all Dirichlet data are to be implemented in the Jacobians and flux variables that appear at boundary nodes. No other steps are needed for the specification of Dirichlet boundary conditions.

Remarks: The FDV equations can be solved using FDM (see example problems in Figure 6.8.2) or FEM. However, the solution process via FEM is much more rigorous. Using the EBE assembly, the maximum size of matrix is 16×16 or 32×32, respectively, for 2-D or 3-D isoparametric elements. The column assembly of EBE strategy combined with GMRES introduced in Section 11.5.3 leads to an expedient solution process. Thus, matrix multiplication must be replaced by the local element equations, which will then be transformed into a global column vector. This allows the finite element equations of the large grid system to be solved with the GMRES scheme effectively.

13.7 EXAMPLE PROBLEMS

(1) Quasi–1-D Supersonic Flows (Euler Equations) with Two-Step GPG

Given: Quasi–one-dimensional rocket nozzle given in Section 6.8.1.

Solution: This problem was solved using 500 linear finite elements with two-step GPG. The computed results are shown to be in good agreement with the analytical solution in Figure 13.7.1.

(2) Two-dimensional Supersonic Flows (Euler Equations) with Two-Step TGM

Given: Geometry and initial and boundary conditions are as shown in Figure 13.7.2a.

Solution: The results of calculations using TGM are shown in Figure 13.7.2b-e. The L_2 norm error convergence history of all variables is shown in Figure 13.7.2f.

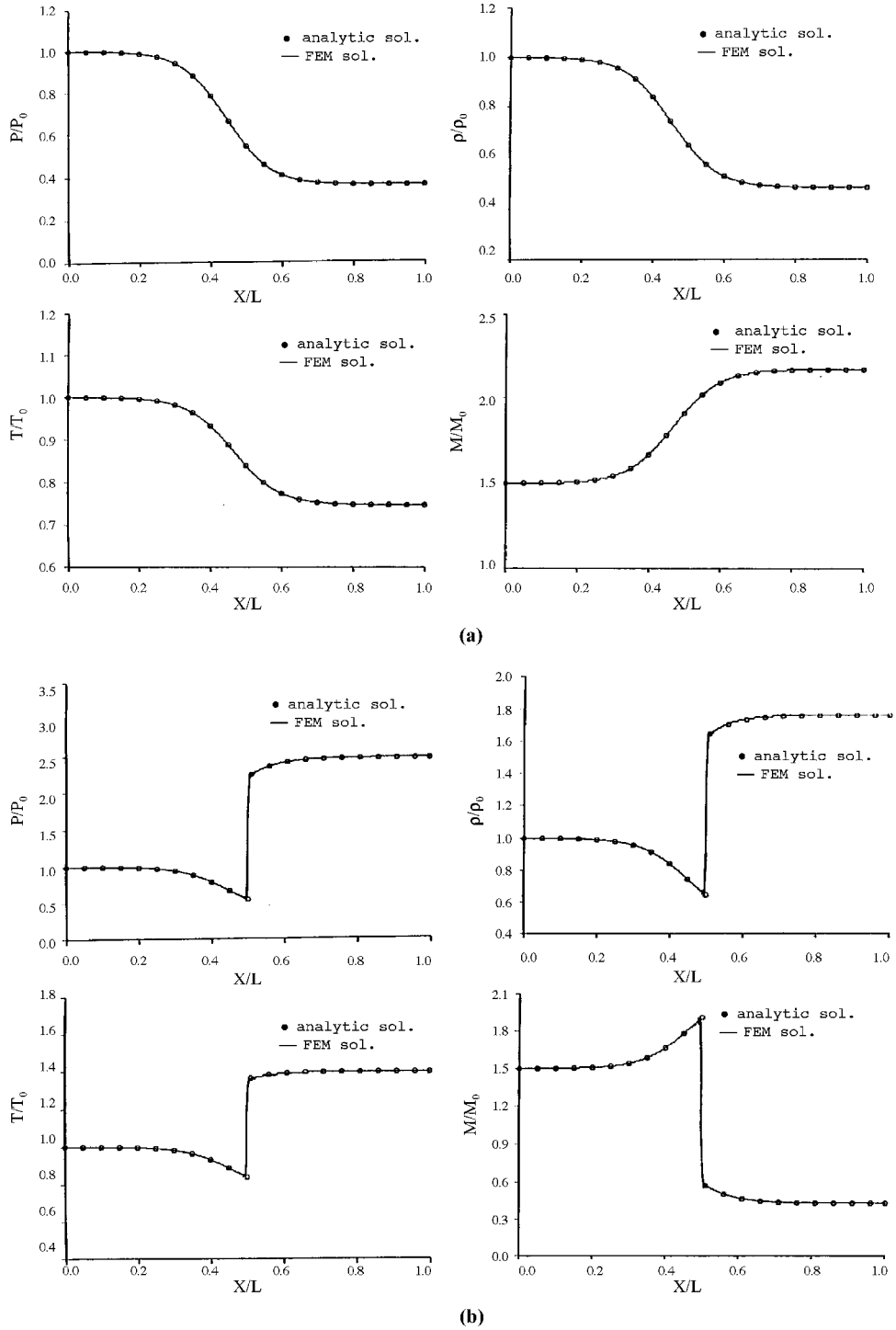

Figure 13.7.1 Quasi–one-dimensional supersonic flow calculations using GPG. **(a)** Supersonic inlet, supersonic outlet. **(b)** Supersonic inlet, subsonic outlet.

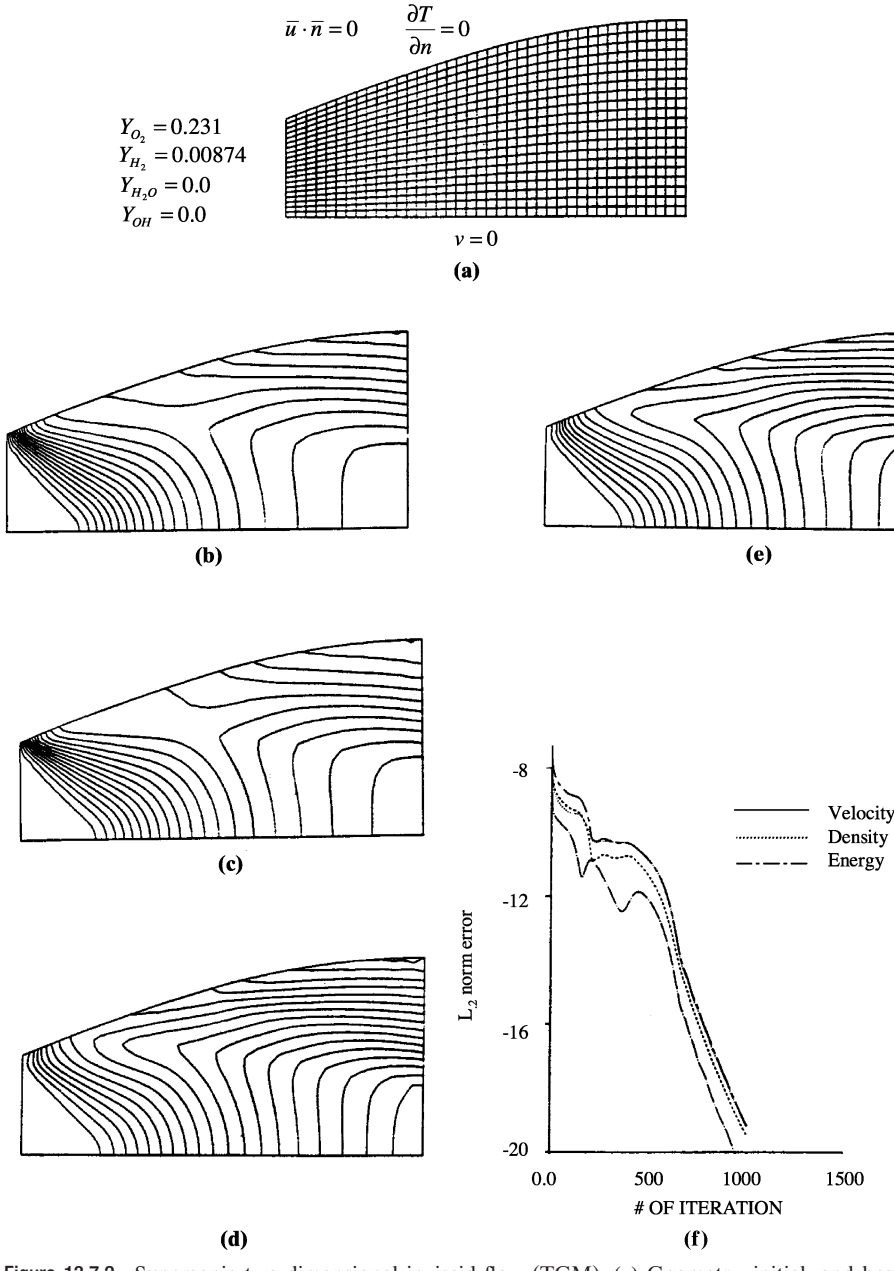

Figure 13.7.2 Supersonic two-dimensional inviscid flow (TGM). **(a)** Geometry, initial, and boundary conditions ($M_\infty = 1.4$, $V_\infty = 1230$m/s, $T_\infty = 1900$K, $P_\infty = 0.81$MPa). **(b)** Density contours. **(c)** Pressure contours. **(d)** Mach number contours. **(e)** Temperature contours. **(f)** Convergence.

(3) Examples for FDV Methods

(a) Shock Tube Problems. Two shock tube problems of differing shock strengths of the following data (AI unit) are tested:

(i) $p_L = 10^5, \quad \rho_L = 1, \quad p_R = 10^4, \quad \rho_R = 0.125$
(ii) $p_L = 10^5, \quad \rho_L = 1, \quad p_R = 10^3, \quad \rho_R = 0.01$

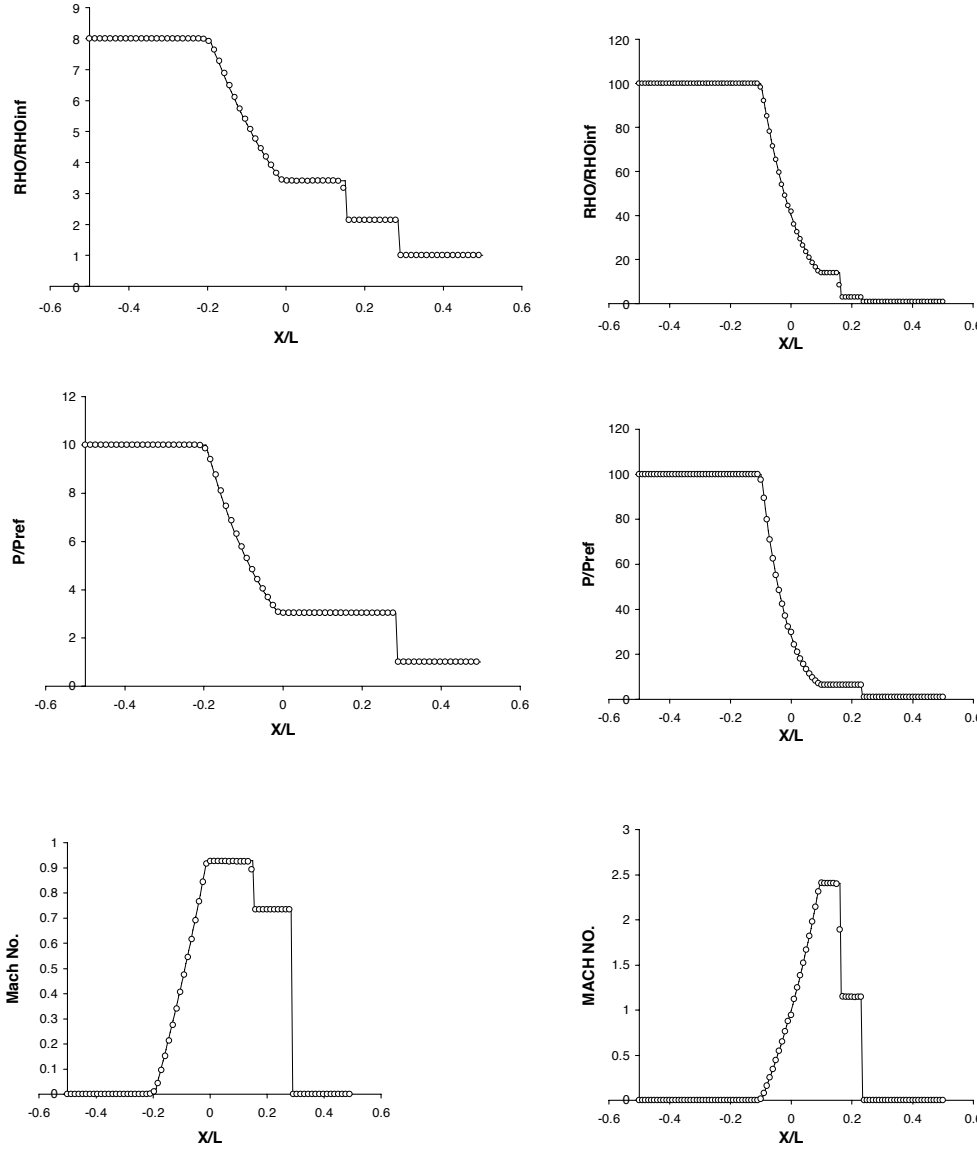

(a) $P_L = 10^5, \rho_L = 1, P_R = 10^4, \rho_R = 0.125,$ $t = 5.2$ ms

(b) $P_L = 10, \rho_L = 1, P_R = 10^{-1}, \rho_R = 0.01,$ $t = 2.65$ ms

Figure 13.7.3.1 Shock tube calculations (1,200 elements) using the FDV theory, solid lines and symbols indicating analytical solutions and numerical results, respectively.

The FDV solutions for the above shock tube cases indicate perfect agreements with the analytical solutions as shown in Figure 13.7.3.1. The advantage of the FDV theory is an automatic switch from the Navier-Stokes system of equations to Euler equations with the calculated diffusion variation parameters (s_3, s_4) being zero everywhere in the domain. Only the convection variation parameters (s_1, s_2) remain nonzero.

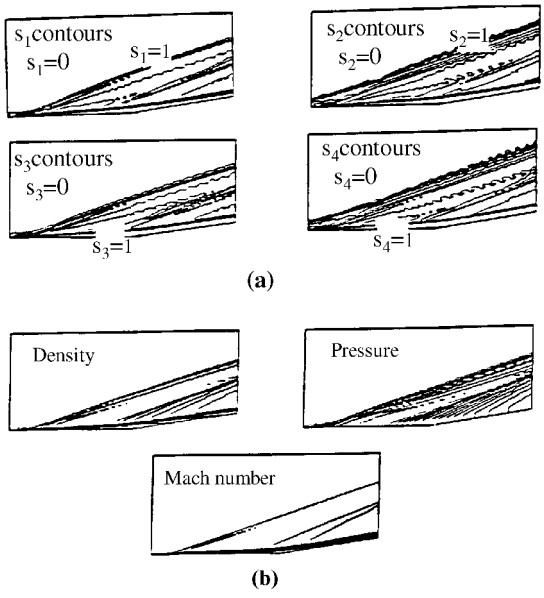

Figure 13.7.3.2 Contour plots of calculated variation parameters to test flow field-dependent properties in FDV. Note that variation parameter contours resemble those of flowfields themselves. **(a)** Calculated variation parameter contour distributions. **(b)** Flowfield contour distributions.

(b) Compression Corner Flows. To demonstrate the role of the variation parameters, we examine the FDV solution for the flow over a ten-degree compression corner at $M_\infty = 3$, $\mathrm{Re} = 1.68 \times 10^4$ (Figure 13.7.3.2). Note that the contour distributions of the first order convection variation parameter s_1 resemble the flowfield depicting the shock waves, as shown in Figure 13.7.3.2a. The second order convection variation parameter s_2 which represents the artificial viscosity for shock capturing closely follows s_1 with somewhat wavy distributions ($s_2 = s_1^{1/4}$). It is seen that the $s_1 = 0$ region (no changes in Mach number) is clearly distinguished from the region near the wall where s_1 is close to unity (rapid changes of Mach number). Note that $s_1 = 0$ changes to $s_1 = 1$ abruptly along the line where the shock is expected to appear.

It is seen that the contour distributions of the first order diffusion variation parameter s_3 resemble the boundary layer formation in the vicinity of the wall with thickening of contours toward the wall as compared to the first order convection variation parameter s_1. The second order diffusion variation parameter s_4 whose role is to provide numerical diffusion for stability for the calculation of fluctuations of turbulent motions follows the trend of s_3 with wavy distributions ($s_4 = s_3^{1/4}$). No change in Reynolds number is indicated by $s_3 = 0$ in the upper upstream region, which coincides with $s_1 = 0$ for convection as expected.

The actual flowfield calculations based on these variation parameters are shown in Figure 13.7.3.2b. As the FDV theory dictates, the first order variation parameters (s_1, s_3) control the physics and accuracy, whereas the second order variation parameters (s_2, s_4) address numerical diffusion for stability. These variation parameters are updated

throughout the computational process until the steady-state is reached, with their contours continuously resembling the actual flowfield.

It should be noted that the physical interactions between inviscid/viscous, compressible/incompressible, and laminar/turbulent flows are simultaneously controlled by the first and second order convection/diffusion variation parameters. These assessments will be verified from additional example problems presented below.

(4) Driven Cavity Flow Problems to Test Compressibility/Incompressibility Characteristics

This example is to demonstrate that the FDV scheme is capable of reaching the incompressible limit at low speeds as well as the shock capturing capability at high speeds. The cavity flow problem [Ghia et al., 1982; Yoon et al., 1998] is examined here for two different Mach numbers ($M = 0.01$ and $M = 0.1$). Streamline and vorticity contours shown in Figure 13.7.4a–d are in good agreement with FDM results of Ghia et al. [1982]. Density distributions (Figure 13.7.4e) for $M = 0.01$ are constant throughout the domain, whereas at $M = 0.1$ we note that variations begin to occur near the downstream upper region. The most significant feature is the distribution

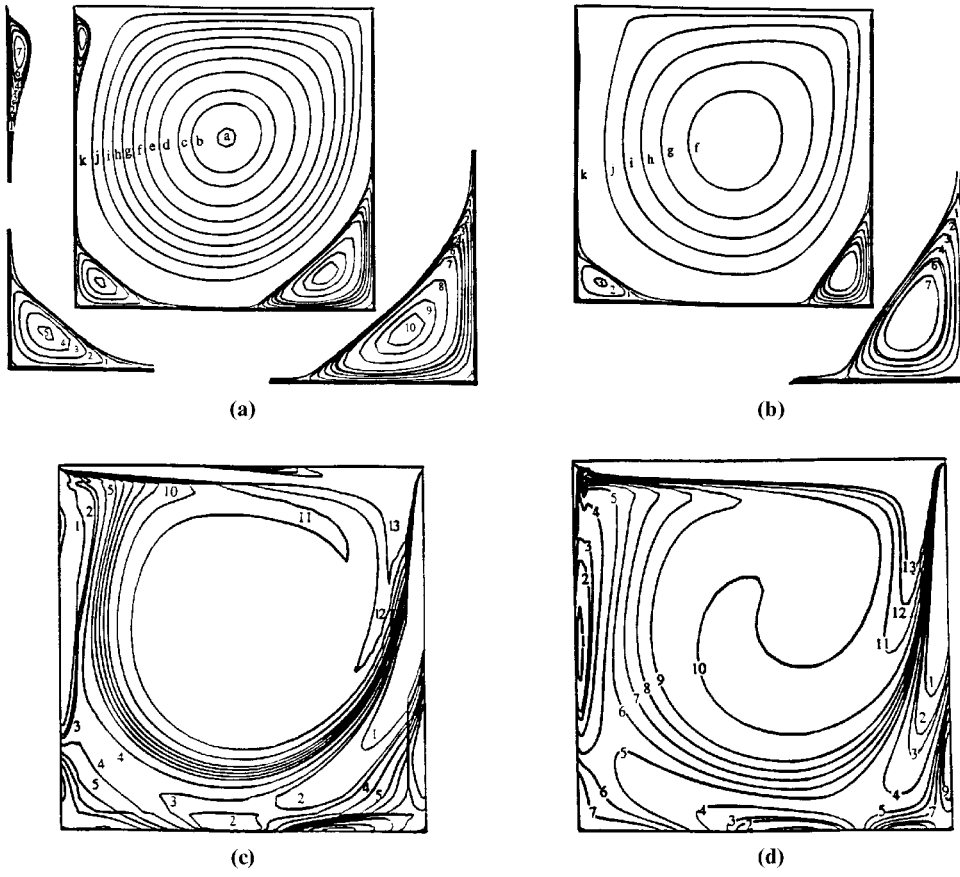

Figure 13.7.4 Driven cavity problems testing incompressibility/compressibility characteristics based on FDV theory. **(a)** Streamlines for $M = 0.01$. **(b)** Streamlines for $M = 0.1$. **(c)** Vorticity contours for $M = 0.1$. **(d)** Vorticity contours for $M = 0.01$.

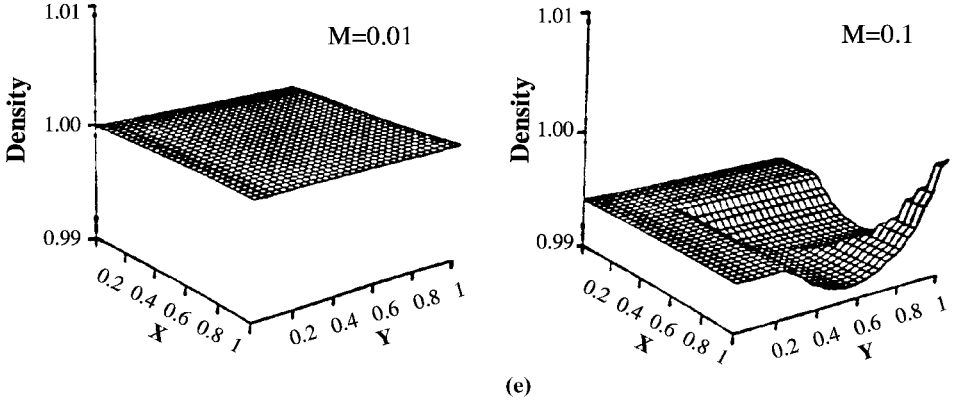

Figure 13.7.4 ***Continued.*** **(e)** Density distributions. **(f)** Stagnation (total) pressure distributions. **(g)** Comparison of velocity distributions with experiments.

of the stagnation (total) pressure (Figure 13.7.4f) as calculated from (6.5.36), indicating that the stagnation pressure is constant at $M = 0.01$ and it begins to vary at $M = 0.1$, almost exactly the same way as density. This proves that (6.5.36) acts as the equation of state encompassing the incompressible and compressible flows. Comparisons of the FDV solutions for the velocity distributions at the centerlines (Figure 13.7.4g) confirm the trend disclosed in Figure 13.7.4e,f. The velocity distributions for $M = 0.01$ are identical to the results of the experimental data for incompressible flow, whereas the solution for $M = 0.1$ (compressible effect present) deviates from the incompressible case. The evidence is overwhelming that the FDV scheme is capable of treating the transition automatically between the incompressible and compressible limit.

(5) Hypersonic Flow Solutions by the FDV Method, $M = 20$, Re = 300,000, with Impinging Shock Wave on a Flat Inlet Combustion Chamber

This example uses the impinging shock wave angle of 12.7° corresponding to the deflection angle of 10°. The solution clearly shows the advantage of the FDV method, with

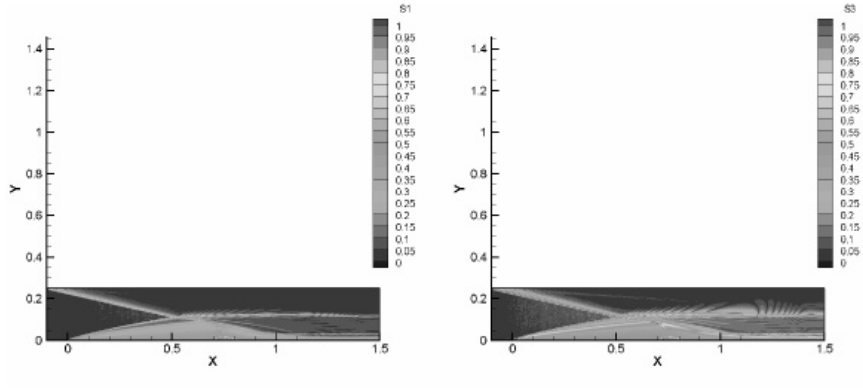

FDV Parameter s_1 FDV Parameter s_3

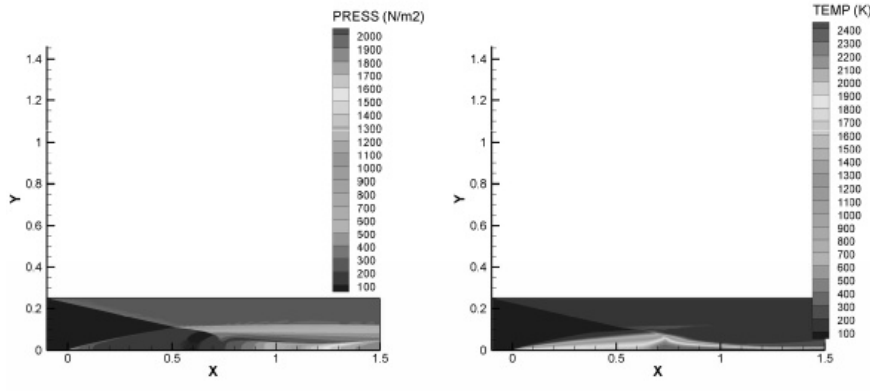

Pressure Contours Temperature Contours

Figure 13.7.5 FDV parameters s_1 and s_2 as calculated from the local Mach numbers and Reynolds numbers resembling the flow field itself.

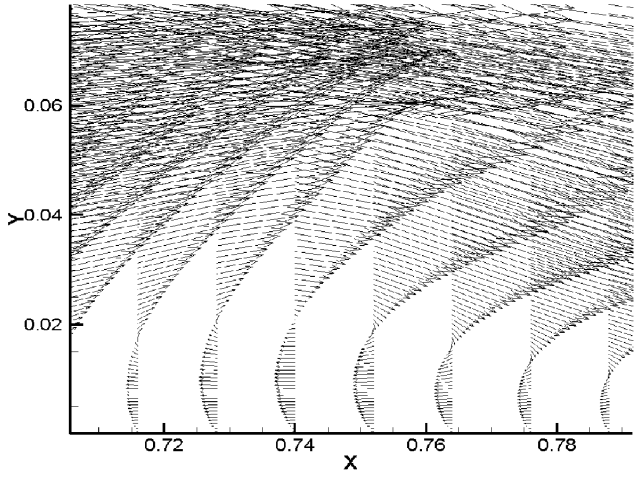

Figure 13.7.6 Velocity vectors near the wall showing the primary and secondary boundary layers and reversed flows.

the FDV parameters s_1 and s_3 guiding the actual flow field topology and the flow field Jacobians dictating the shock wave turbulence boundary layer interactions. Furthermore, the primary and secondary boundary layers are shown clearly with the reverse and rotational flows close to the walls (Figures 13.7.5–13.7.7). No chemical reactions are considered in this solution. See Chapter 22 for detailed discussions on chemical reactions. The results in this example were obtained from the computer program developed by Gary Heard.

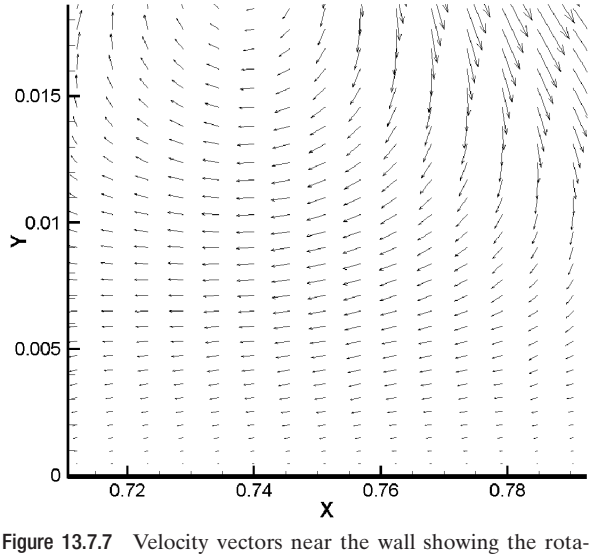

Figure 13.7.7 Velocity vectors near the wall showing the rotational flow.

13.8 SUMMARY

In this chapter, most of the currently available compressible flow analyses using FEM have been presented. They include GGM (generalized Galerkin methods), TGM (Taylor-Galerkin methods), GPG (generalized Petrov-Galerkin methods), CGM (characteristic Galerkin methods), DGM (discontinuous Galerkin methods), and FDV (flowfield-dependent variation methods). Exhaustive numerical results on TGM and GPG are available in the literature, and no attempt is made to introduce them here. Only a few selective examples are shown in Section 13.7 for illustration.

Transitions and interactions between inviscid/viscous, compressible/incompressible, and laminar/turbulent flows can be resolved by the FDV theory. It is shown that the FDV parameters initially introduced in the Taylor series expansion of the conservation variables of the Navier-Stokes system of equations are translated into flowfield-dependent physical parameters responsible for the characterization of fluid flows. In particular, the convection FDV parameters (s_1, s_2) are identified as equivalent to the TVD limiter functions. The FDV equations are shown to contain the terms of fluctuation variables automatically generated in due course of developments, varying in time and space, but following the current physical phenomena. In addition, adequate numerical controls (artificial viscosity) to address both nonfluctuating and fluctuating parts of variables are automatically activated according to the current flowfield. Just as important are the Jacobians providing interactions of any one variable with all other variables in the conservation form of the governing equations. It has been shown that practically all existing numerical schemes in FDM and FEM are the special cases of the FDV theory.

Some simple example problems have demonstrated most of the features available in the FDV theory. It was shown that the calculated FDV parameters resemble the flowfield itself. The program originally designed for the solution of the supersonic flows is used to resolve incompressible flows of driven cavity problems, with the transition from incompressibility to compressibility automatically realized.

There are other methods related to FEM which are not introduced in this chapter. They include spectral element methods, least square methods, and finite point methods. These are the subjects of the next chapter.

REFERENCES

Aliabadi, S. K. and Tezduyar, T. E. [1993]. Space-time finite element computation of compressible flows involving moving boundaries. *Comp. Meth. Appl. Mech. Eng.*, 107, 209–23.

Atkins, H. L. and Shu, C. W. [1998]. Quadrature-free implementation of discontinuous Galerkin method for hyperbolic equations. *AIAA J.*, 36, 5, 775–82.

Baumann, C. E. and Oden, J. T. [1999]. A discontinuous *hp* finite element methods for the Euler and Navier-Stokes equations. *Int. J. Num. Meth. Fl.*, 31, 79–95.

Boris, J. P. and Book, D. L. [1976]. Solution of the continuity equation by the method of flux corrected transport. *J. Comp. Phys.*, 16, 85–129.

Choi, D. and Merkle, C. L. [1993]. The application of preconditioning for viscous flows. *J. Comp. Phys.*, 105, 203–23.

Chung, T. J. [1999]. Transitions and interactions of inviscid/viscous, compressible/incompressible and laminar/turbulent flows. *Int. J. Num. Meth. Fl.*, 31, 223–46.

Cockburn, S., Hou, S., and Shu, C. W. [1990]. TVD Runge-Kutta local projection discontinuities Galerkin finite element for conservation laws, IV. The multidimensional case. *Math. Comp.* 54–65.

——— [1997]. The Runge-Kutta discontinuous Galerkin method for conservation laws. V. Multidimensional systems. ICASE Report 97–43.

Codina, R., Vazquez, M., and Zienkiewicz, O. C. [1998]. A general algorithm for compressible and incompressible flows. Part III: The semi-implicit form. *Int. J. Num. Meth. Fl.*, 27, 13–32.

Ghia, U., Ghia, K. N., and Shin, C. T. [1982]. High-Reynolds number solutions for incompressible flow using the Navier-Stokes equations and Multigrid method. *J. Comp. Phys.*, 48, 387–411.

Godunov, S. K. [1959]. A difference scheme for numerical computation of discontinuous solution of hydrodynamic equations. *Math. Sbornik*, 47, 271–306.

Harten, A. [1983]. On the symmetric form of systems of conservation laws with entropy. *J. Comp. Phys.*, 49, 151–64.

——— [1984]. On a class of high resolution total variation stable finite difference schemes. *SIAM J. Num. Anal.*, 21, 1–23.

Hassan, O., Morgan, K., and Peraire, J. [1991]. An implicit explicit element method for high-speed flows. *Int. J. Num. Meth. Eng.*, 32(1): 183.

Hauke, G. and Hughes. T. J. R. [1998]. A comparative study of different sets of variables for solving compressible and incompressible flows. *Comp. Meth. Appl. Mech. Eng.*, 153, 1–44.

Hughes, T., Franca, L., and Mallet, M. [1986]. A new finite element formulation for computational fluid dynamics: I. Symmetric forms of the compressible Euler and Navier-Stokes equations and the second law of thermodynamics. *Comp. Meth. Appl. Mech. Eng.*, 54, 223–34.

Johnson, C. and Pitkäranta, J. [1986]. An analysis of the discontinuous Galerkin method for a scalar hyperbolic equation. *Math. Comp.*, 46, 173, 1–26.

LaSaint, P. and Raviart, P. A. [1974]. On a finite element method for solving the neutron transport equations. In C. deBoor (ed.) *Mathematical Aspects of Finite Elements in Partial Differential Equations*. New York: Academic Press.

Oden, J. T., Babuska, I., and Baumann, C. [1998]. A discontinuous *hp* finite element method for diffusion problems. *J. Comp. Phys.*, 146, 491–519.

Osher, S. [1984]. Rieman solvers, the entropy condition and difference approximations. *SIAM J. Num Anal.*, 21, 217–35.

Richardson, G. A., Cassibly, J. T., Chung, T. J., and Wu, S. T. [2010]. Finite element form of FDV for widely varying flowfilds. *J. of Com. Physics*, 229, 149–167.

Roe, P. L. [1984]. Generalized formulation of TVD Lax–Wendroff schemes. ICASE Report 84–53. NASA CR-172478, NASA Langley Research Center.

Schunk, R. G., Canabal, F., Heard, G. A., and Chung, T. J. [1999]. Unified CFD methods via flowfield-dependent variation theory, AIAA paper, 99–3715.

Shakib, F., Hughes, T., and Johan, Z . [1991]. A new finite element formulation for computational fluid dynamics: X. The compressible Euler and Navier-Stokes equations. *Comp. Meth. Appl. Mech. Eng.*, 89, (1–3): 141–220.

Tadmor, E. [1984]. The large time behavior of the scalar, genuinely nonlinear Lax-Friedrichs scheme. *Math. Comp.*, 43, 353–68.

Van Leer, B. [1979]. Towards the ultimate conservative difference scheme. V. A second order sequel to Godunov's method. *J. Comp. Phys.*, 32, 101–36.

Yoon, K. T. and Chung, T. J. [1996]. Three-dimensional mixed explicit-implicit generalized Galerkin spectral element methods for high-speed turbulent compressible flows. *Comp. Meth. Appl. Mech. Eng.*, 135, 343–67.

Yoon, K. T., Moon, S. Y., Garcia, S. A., Heard, G. W., and Chung, T. J. [1998]. Flowfield-dependent mixed-implicit methods for high and low speed and compressible and incompressible flows. *Comp. Meth. Appl. Mech. Eng.*, 151, 75–104.

Zalesak, S. T. [1979]. Fully multidimensional flux corrected transport algorithm for fluids. *J. Comp. Phys.*, 31, 335–62.

Zienkiewicz, O. C. and Codina, R. [1995]. A general algorithm for compressible and incompressible flows – Part I. The split characteristic based scheme. *Int. J. Num. Meth. Fl.*, 20, 869–85.

Zienkiewicz, O. C., Satya Sai, B. V. K., Morgan, K., and Codina, R. [1998]. Split, characteristic based demi-implicit algorithm for laminar/turbulent incompressible flows. *Int. J. Num. Meth. Fl.*, 23, 787–809.